Histological evaluation of bone metabolism discrepancies resulting from Neuroligin 3 and 4 Knockout in Autistic Mouse Model

Inauguraldissertation

zur Erlangung des Grades eines Doktors der Medizin

des Fachbereichs Medizin

der Justus-Liebig-Universität Gießen

vorgelegt von Julia Janine Glaser

aus Karlsruhe

Gießen 2025

Aus dem Fachbereich Medizin der Justus-Liebig-Universität Gießen

Labor für Experimentelle Unfallchirurgie der Klinik und Poliklinik für Unfall-, Hand- und Wiederherstellungschirurgie

Gutachter: Prof. Dr. rer. nat. Thaqif El Khassawna

Gutachter: PD Dr. med. Klaus Deckmann

Tag der Disputation: 14.01.2025

Inhaltsverzeichnis

1. Introduction

Autism spectrum disorder (ASD) is a neurodevelopmental condition primarily known for impairing social interaction and causing repetitive behaviors and interests (1). Although not traditionally linked to trauma surgery, recent studies (2,3), have reported a higher incidence of bone fractures and injuries in both pediatric and adult ASD populations. Thus, beyond its impact on mental health and motor skills, ASD may also affect bone metabolism.

Bone's role in maintaining overall body homeostasis is well-established (4). However, the immune system's contribution to bone health, particularly in the context of ASD, remains underexplored. Previous research has demonstrated the critical role of the immune system in bone healing (5). This thesis uses immune- and enzymatic histochemistry to investigate immune system involvement in an autistic mouse model.

The research focuses on the radiological and histological evaluation of bone in both normal adolescent mice and genetically modified knockout mice within an established ASD model.

The lack of foundational research exploring the relationship between neurodevelopmental disorders and bone metabolism highlights the novelty of this study. The primary goal is to identify and demonstrate cellular-level differences, providing a basis for further preclinical investigations. This research aims to explore potential approaches to improving bone structure in ASD patients.

2. Theoretical background

2.1. Bone

The human musculoskeletal system is divided into active and passive parts. The active part includes skeletal muscles that can be moved voluntarily. The passive part consists of bones, tendons, and ligaments that form the skeletal structure and joints (6). The primary functions of the musculoskeletal system include support and stabilization, movement of body parts like arms and legs, and protection of internal organs such as the brain and bone marrow.

Due to constant compressive, tensile, and bending stress, bones undergo continual remodeling to adjust to mechanical loads (6). Another major role of bones is regulating calcium balance and blood formation (7).

Macroscopic bone structure

While all human bones share a similar elementary structure, their macroscopic forms vary. There are long, short, flat, air-filled, and irregular bones (6). For instance, the femur is a long bone, the carpal bones are short bones, the scapula and sternum are flat bones, the sphenoid and frontal bones are air-filled, and vertebrae and the mandible are irregular bones (8).

The periosteum, a connective tissue layer, covers the outermost bone layer. It consists of two sections: the stratum fibrosum and the stratum osteogenicum. The stratum fibrosum contains collagen fibers, including Sharpey's fibers, which extend into the cortical bone and serve as attachment points for tendons and ligaments. The stratum osteogenicum contains stem cells that can differentiate into osteoclasts and osteoblasts, essential for bone remodeling and fracture healing. This layer also houses blood vessels, capillaries, and nerve terminals, contributing to the periosteum's pain sensitivity (6).

Beneath the periosteum lies a thin layer of compact bone, known as cortical bone. In long bones, particularly in the diaphysis, this layer is thickest and is called the substantia compacta. The cancellous bone, located within the cortical bone, consists of trabeculae and forms the substantia spongiosa, which undergoes continuous reconstruction based on mechanical stress (6).

Bone marrow resides in the cavities of the trabeculae. Its composition varies with location and age. Red bone marrow, found in the epiphyses of long bones and flat bones like the sternum and ribs, is responsible for blood formation. In the diaphysis of long bones, yellow bone marrow, composed predominantly of adipose tissue, does not actively contribute to hematopoiesis (7,8). The endosteum, the innermost layer, envelops the cortical bone and trabeculae and contains stem cells for bone progenitor cell differentiation (6).

Microscopic anatomy of the bone

Microscopically, bone is divided into lamellar bone and woven (non-lamellar) bone (7). Lamellar bone, found in normal adult bone, consists of collagen fibers arranged in parallel layers and bundles. In cortical bone, lamellar bone forms osteons and Harvesian systems, with osteons communicating with the medullary cavity through Volkmann's canals (6). In cancellous bone, trabeculae are oriented according to mechanical stress. Woven bone, found in areas of fracture healing, tendon or ligament attachments, and pathological conditions (9), has randomly arranged collagen fibers. It is mechanically weaker than lamellar bone and usually remodels into lamellar bone over time. (7).

In their mature form, bones primarily consist of lamellar bone tissue. Lamellae form osteons that arrange in groups around the Canalis centralis (Harversian canal) in cortical bone, reaching lengths up to 0.5 to 1.0 cm. Volkmann's canals enable communication among osteons. The skeletal framework constantly undergoes remodeling, precluding its classification as a static system (6).

Bone composition / Bone at cellular level

Bone consists of four major cell types: osteoblasts, bone lining cells, osteoclasts, and osteocytes (10). Each of them plays an important role in the process of bone remodelling. Each cell type plays a crucial role in bone remodeling. Understanding the interplay among these cells is essential to comprehending bone formation and remodeling processes. (Figure 1).

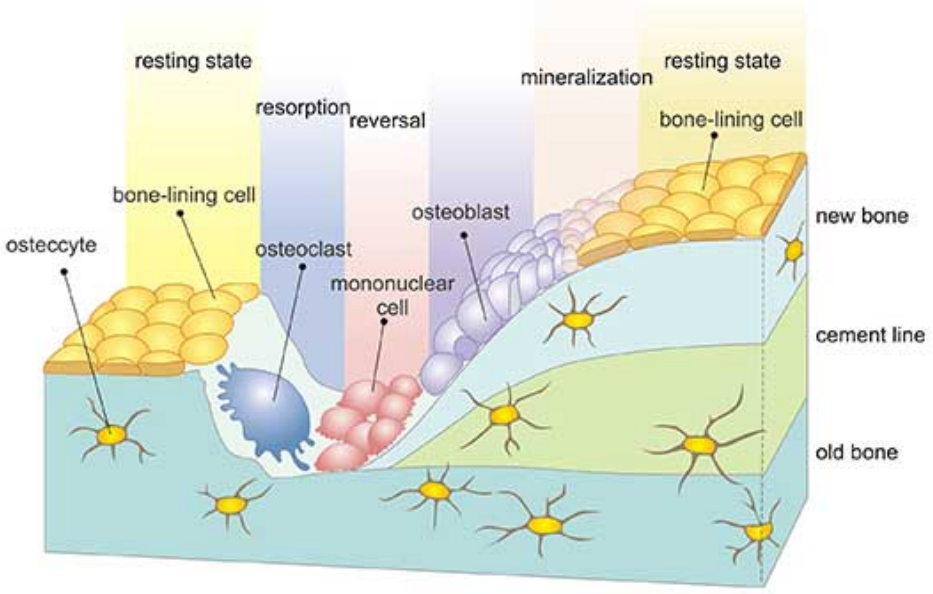

Figure 1: Schematic illustration of Bone Remodelling. Osteocytes are present in both older and newly formed bone layers. Bone lining cells, osteoblasts, and osteoclasts are located on the surface of the bone. During the resorption phase, osteoclasts

predominate, while during the bone formation phase, osteoblasts prevail. In the resting state, bone lining cells are predominantly found on the surface. Copywrite, 2020, Tresguerres et al. (11).

Osteoblasts

Osteoblasts are derived from pluripotential mesenchymal stem cells and are not surrounded by bone matrix. As a result, they are located only on the surface of the bone. Osteoblasts activate osteoclast progenitor cells and produce osteoid, the non-mineralized bone matrix (10).

Bone-lining cells

Bone-lining cells are the immediate precursors of osteoblasts (12). They are found lining the bone-forming surface, near active osteoblasts. These cells interact with Haversian canals and may serve as a 'cell-barrier,' controlling ion fluxes between mineralized and non-mineralized areas (10).

Osteoclasts

Osteoclasts are multi-nucleated scavenger cells typically attached to the bone surface. Originating from hematopoietic stem cells, matured monocytes and macrophages can differentiate into active osteoclasts (13). They are located in extensive areas called 'Howship's lacunae,' where their primary role is bone resorption (14). Osteoclasts also induce mesenchymal stem cells and osteoblasts to initiate bone remodeling (15).

Osteocytes

Osteocytes are former osteoblasts entirely surrounded by mineralized bone matrix or trapped within lacunae. They are interconnected via dendritic connections through canaliculi and constitute 90-95% of all bone cells (10, 14). Recently, osteocytes were discovered to have an endocrine function, secreting sclerostin, which regulates bone mass formation, and FGF-23, an important regulator of phosphate metabolism. Osteocytes also function as mechanosensory cells, transmitting mechanical signals into chemical ones to inform osteoblasts and osteoclasts (11).

Extracellular Matrix

Bone comprises cells and an extracellular matrix. The organic part constitutes 35% of the matrix, primarily composed of type 1 collagen (90%), non-collagenous proteins, proteoglycans, glycosaminoglycans, and lipids. The inorganic part (65%) consists

primarily of hydroxyapatite $Ca_5(OH)(PO_4)_3$ (10). Osteoblasts synthesize Type 1 collagen as a procollagen molecule, which is distinguished by strong covalent crosslinks. This procollagen molecule features a triple helical structure (10). Non-collagenous proteins like alkaline phosphatase, osteocalcin, and osteonectin are crucial for matrix mineralization. These proteins also regulate the metabolism of osteoblasts and osteoclasts (10).

Bone Multicellular Unit

The bone undergoes continuous architectural changes through the coordinated activity of a group of cells known as the "bone multicellular unit" (BMU) (10). This group includes osteoclasts, osteoblasts, and their progenitor cells. Initially, osteoclasts resorb bone matrix in a specific region. Mononuclear cells then complete the resorption process. Osteoblasts subsequently migrate to form new bone matrix. Following the 'osteoid maturation time,' the bone is replaced by new mineralized bone matrix. During this process, some osteoblasts become enclosed within the matrix and transition to osteocytes. This interconnected process of bone resorption and formation maintains normal bone structure (6,10).

2.2. The immune system

The immune system consists of cells, molecules, and mechanisms that coordinate defensive responses to foreign microbes and substances upon exposure. Its primary task is defending against infections induced by microorganisms. The immune response is divided into two parts: the innate immune system, which provides an early and rapid response within hours, and the adaptive immune system, which offers a more specialized response that develops within days of infection. The different cell types involved in immune reactions are illustrated in Figure 2.

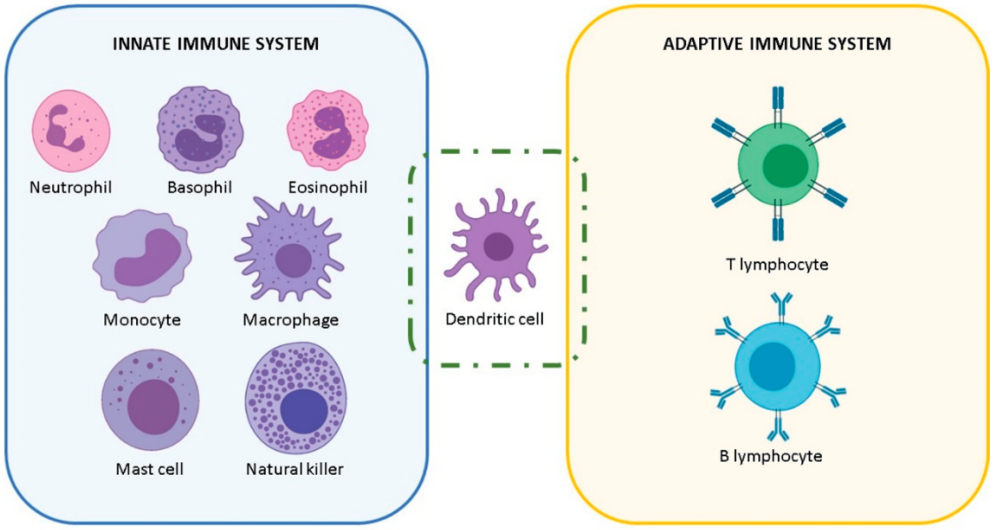

Figure 2: Innate and adaptive immunity. The innate immune system consists of various cells capable of mounting a rapid immune response against pathogenic microorganisms. On top of this initial immune response, the adaptive immune system provides the ability, after adapting to the pathogenic microorganisms, to enable a more specific immune response for final elimination. In between, dendritic cells are found, which initiate and regulate the antigen-specific immune response. Copywrite, 2021, Ernst et al (16).

Innate immune System

The immune system includes a native immunity, known as the innate immune system, which can react quickly to foreign elements. This initial response is crucial for protecting the body and offers various reaction mechanisms. Physical barriers, such as the ciliated epithelium of the lungs, and chemical barriers, like gastric acid in the stomach, prevent pathogens from penetrating the body (17,18).

Additionally, phagocytic cells (macrophages, natural killer cells, and neutrophils), complement system activation, and cytokine secretion characterize the innate immune system (17,18). However, innate immunity may not always be sufficient to prevent microbes from breaching these barriers, necessitating the involvement of the adaptive immune system to eliminate pathogenic germs effectively (17).

Adaptive immune System

The adaptive immune system provides a more specialized response than the innate immune system, resulting in a more effective defense against pathogens. This response takes longer to develop but operates in a more specific and targeted manner. The adaptive immune system relies heavily on innate immunity and antigen presentation. The

cells involved in adaptive immunity are B- and T-cell lymphocytes, which can be divided into humoral and cell-mediated immunity. Both aim to reduce and eliminate antigens. Humoral immunity involves the secretion of antibodies by B-lymphocytes, leading to the phagocytosis of microbes. Cell-mediated immunity is controlled by T-lymphocytes, which initiate lysis and phagocytosis by activating macrophages.

2.3. Cells of the Immune System

Different cell types play crucial roles in the immune response. These include monocytes, macrophages, and neutrophils in the innate immune system and B- and T-cell lymphocytes in the adaptive immune system.

Monocytes & macrophages

Monocytes and macrophages are integral components of the innate immune system. Originating from immature lymphocytes, their primary role is immune defense through phagocytosis, making them part of the mononuclear phagocyte system (MPS) (17,18). Monocytes originate from myeloid progenitor cells, which themselves are derived from pluripotent hematopoietic stem cells. As granulocytic cells, monocytes exist in the peripheral blood as incompletely differentiated cells until they are activated and mature into macrophages. The maturation process continues as monocytes differentiate into macrophages in the bloodstream and migrate to various tissues throughout the body.
Macrophages are found in all organs and are named according to their tissue location, such as Kupffer cells in the liver and osteoclasts in bone. Particularly, macrophages secrete mediators that stimulate osteoclastic bone resorption.

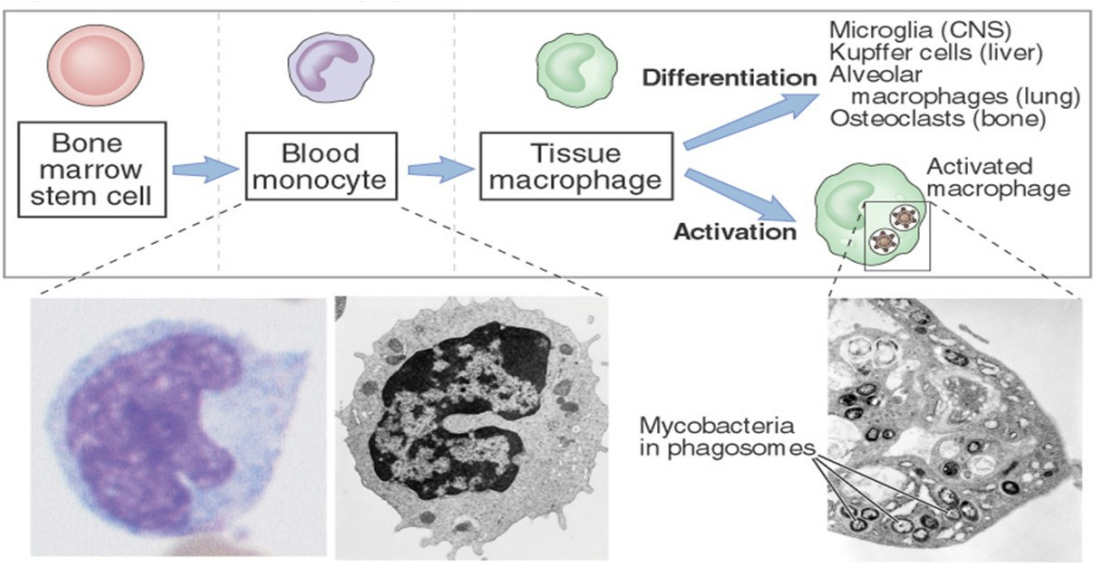

Figure 3: Maturation of mononuclear phagocytes. Arising from bone marrow stem cells, tissue macrophages differentiate from monocytes. Depending on their specific tasks, they further differentiate into tissue-specific forms (such as microglia cells in the central nervous system). When activated, they can undertake their function in the immune system through phagocytosis. Copywrite 2001, Janeway (18).

The primary function of these cells, as part of the MPS, is phagocytosis. They display antigens for T-lymphocytes to activate the adaptive immune system and secrete cytokines to activate proinflammatory cells.

Macrophages not only initiate proinflammatory processes but also support tissue homeostasis by removing dead cells and aiding in cell repair. Additionally, they regulate immunomodulation by producing both pro-inflammatory and anti-inflammatory signals. These phagocytic cells can be divided into M1 and M2 macrophages. M1 cells are primarily involved in the pro-inflammatory response by releasing cytokines such as TNF-alpha, IL-6, and IFN-gamma to initiate regeneration processes. M2 macrophages elicit a predominantly anti-inflammatory response, which is essential for tissue remodeling and enchondral ossification in the bone (5,19). Impaired macrophage function affects healing processes in bone fractures, particularly in enchondral ossification, leading to delayed maturation of cartilage stages in bone formation (20,21).

B- and T- cells/lymphocytes

B- and T-lymphocytes, along with natural killer cells, descend from pluripotent hematopoietic stem cells through a lymphoid progenitor. B-cells evolve into plasma cells after activation and are responsible for producing and secreting antibodies. T-cells, as

effector cells of cell-mediated immunity, differentiate into cytotoxic T-cells and helper T-lymphocytes. After antigenic stimulation, the cells secrete cytokines to control and regulate the maturation and differentiation of other T- and B-cells, regulate the inflammatory response, and activate macrophages.

2.4. Autism Spectrum disorder

Definition

Patients with Autism Spectrum Disorder (ASD) exhibit significant abnormalities in social interaction and communication, characterized by repetitive, stereotypical behavior (22). From childhood, they display lifelong symptoms such as difficulties with routine transitions and understanding or expressing emotions. The severity and clinical presentation of symptoms are heterogeneous. Currently, there are no curative treatments for this pervasive developmental disorder, but symptom alleviation and improvement are possible. The classic autistic triad includes qualitative impairments in interpersonal interaction, communication, and restricted, stereotyped interests and activities (22,23).

In the Diagnostic and Statistical Manual of Mental Disorders (DSM-V), ASD encompasses early infantile autism, Asperger's Syndrome, and atypical autism (PDD-NOS = pervasive developmental disorder – not otherwise specified) (23).

Epidemiology

Over the past decades, diagnostic instruments and classifications have evolved, resulting in discrepancies between studies and methods, making it challenging to determine incidence or prevalence (22).

Most studies estimate an average prevalence of 62 per 10,000, meaning 1 in 160 children suffers from ASD. Additional population-based research indicates a higher incidence, suggesting a prevalence rate of approximately 0.9% to 1.1% (24). The gender distribution indicates that ASD is more prevalent in males than in females, with a ratio of four males affected for every female (1).

Recent years have seen an increase in ASD diagnoses, particularly in children: from 0.22% in 2007 (males: 0.3%; females: 0.14%) to 0.38% in 2012 (males: 0.54%; females: 0.2%). This increase may be due to improved mental health access, better diagnosis, more educational work, and a real increase in cases. However, the collective of ASD patients has indeed increased (22,24).

Paradoxically, the number of adults diagnosed with ASD is significantly lower than that of children, despite the disease being incurable and patients having an approximately normal life expectancy (22).

Aetiology

ASD is influenced by both environmental and genetic factors (22). Qiu et al. recently investigated an association between genetic variants and ASD risk in an umbrella review of systematic analyses and meta-analyses (25) .

Twin studies indicate that genetic factors, such as mutations, are crucial for ASD pathogenesis. Consequently, structural and functional changes affect patient interaction and communication. Environmental factors, such as higher maternal age, stress, or lack of vitamins during pregnancy, are part of ongoing controversial studies. Physical illness, brain damage, biochemical anomalies, and neuropsychological and neurocognitive deficiencies are also considered (22).

The phenotypic heterogeneity of ASD suggests high genetic variability, complicating the detection of relevant genes, which are organized in a complex inheritance model. Genes such as Neuroligin 3 and 4 (NLGN3, NLGN4), Neurexin 1 (NRXN1), SHANK3, and the Oxytocin receptor gene (OXTR) may interact in this model (22,26).

Neuroligin 3 and 4

NLGN3 and NLGN4 are crucial proteins in synaptogenesis (22) and synaptic transmission. Located on the human X chromosome (NLGN3 on Xq13 and NLGN4 on Xp22.32-p22.31) (27). Mutations in these genes cause a knockout and monogenetic neuronal malfunction. NLGN4 deletions in mice cause autism-related behavioral impairments (28), and Neuroligin is identified as an important regulator of social behavior in other models (29).

The Simons Foundation Autism Research Initiative (SFARI) lists various risk genes related to ASD, including NLGN3 and NLGN4 (13,14).

Pathophysiology

The pathophysiological origins of ASD remain under-researched. Discrepancies in brain areas of autistic patients compared to non-affected individuals justify ASD as a brain dysfunction. Abnormalities have been observed in imaging studies of the amygdala, basal ganglia, and corpus callosum (22). Other studies indicate disruptions in serotonergic and dopaminergic systems in affected patients (30).

Symptoms

The symptoms of ASD vary widely among individuals. Key characteristics include: 1) qualitative impairment in interpersonal interactions, such as reduced or inconsistent eye contact, 2) qualitative abnormalities in communication, including diminished facial expressions and gestures, and 3) restricted, stereotypical, and recurring personal interests and activities, leading to an extreme fear of changes. These symptoms manifest in early infancy, typically by age five, and are persistent and incurable, though appropriate therapy can reduce symptoms (22,31).

Course of disease

The progression of ASD varies significantly among individuals, influenced by factors such as individual support, social environment, and therapy. Conspicuous behaviors and anomalies are noticeable from childhood. Autism-specific therapy and increased parental understanding can improve social interaction and reduce symptoms (22). Nonetheless, challenges persist, and adulthood is often marked by significant symptom reduction (32). Cognitive and communicative abilities, such as a higher IQ or better verbal skills, correlate with a favorable prognosis.

Diagnostics

According to ICD-10 and DSM-V criteria, diagnosis is based on qualitative impairments in social interaction and communication, along with restricted interests and stereotypical behaviors, such as repetitive movements and resistance to change. Additional issues, such as phobias, sleep disorders, or aggression, often accompany ASD. Typically, clinical manifestation occurs before the third year of life (22,24).

However, there is no established cellular, genetic marker, or neuropsychological test for early ASD diagnosis, which cannot be reliably made before 18 months of age (1,22).

Therapy

Early intervention, ideally starting in preschool, aims to encourage appropriate behavior and reduce unpleasant behavior. Enhancing social awareness and self-management of emotions can alleviate symptoms. While there is no primary pharmacological treatment for ASD, medications may be considered for additional issues such as sleep disturbances, anxiety, or aggression. (33).

Prognosis

ASD affects personality, social integration, and career opportunities. The disease course and progression depend heavily on individual manifestations. While a cure is impossible,

adequate therapy can improve quality of life. Most affected individuals require lifelong support from their social environment, and there are controversial discussions about a potentially shortened life expectancy (22).

Orthopedic background

Several studies suggest an increased bone fracture rate in children and adults with ASD (3,27). Children with ASD often show lower bone mineral content and reduced cortical area, thickness, and strength at the distal radius and tibia compared to typically developing children. They also exhibit deficits in areal bone mineral density at various skeletal sites and potential impairments in bone mineral content, microarchitecture, and strength (35).

3. Objectives and hypothesis of this study

Children with ASD exhibit a higher incidence of fractures (34). Additionally, lower bone density has been observed in adolescents and younger adults with ASD (3,36). However, no cellular or metabolic explanations have been provided to elucidate these findings. Given the significant increase in the incidence of ASD (37), analyzing causative factors could offer affected individuals an opportunity to enhance their quality of life by preventing such complications. To address this, a deeper understanding of bone metabolism and the role of the immune system is necessary, particularly considering its implicated involvement in ASD (38–40).

The Neuroligin 3 and 4 knockout model is a well-established approach for studying ASD in mouse models (28,29). This genetic anomaly has been observed in both humans and mouse models. Previous studies have demonstrated behavioral alterations resembling characteristics of ASD and identified monogenetic causes of autism through 'loss-of-function mutations in postsynaptic cell-adhesion molecules' (28, 41). Additionally, the use of the C57BL/6J mouse model aged 10-12 weeks has been extensively investigated and proven as a suitable small animal model for ASD research (42).

This thesis examines the discrepancies in cellular bone metabolism between two knockout groups (NL3-/y and NL4-/y) and a wild-type group. Histological and immunohistochemical stainings were performed on samples of mice femora, and bone density analysis was conducted. Differences in cellular, immunological, and histomorphometric levels are evaluated.

Based on these premises, the following hypotheses are formulated:

1. Autism spectrum disorder-associated Neuroligin 3 and 4 knockouts have a significant adverse impact on qualitative and quantitative bone metabolism.
2. Cellular and metabolic discrepancies, shown in immunohistochemical staining and bone density analysis, lead to impaired bone structure.
3. Macrophages, as part of the immune system, exhibit different characteristics in the knockout and wild-type models.

4. Materials and methods

4.1. Experimental animals

The animals used in this small animal model were from the well-known C57BL/6J research model established in 1921 (43,44). This genetic background is the most widely used strain in biomedical research. The C57BL/6J strain is preferable over other subgroups, such as C57BL/6N, where mice frequently go blind after a few months, potentially compromising behavior-based research (45). The Max Planck Institute for Experimental Medicine's Molecular Neurobiology research group in Göttingen provided the experimental animals. The following experiments and investigations were conducted in Gießen (Animal experiment number G35/5423).

4.2. Animal testing assessment

This project is based on an animal model, and a final assessment was made to evaluate the breeding line and abnormalities compared to non-transgenic mice. The evaluation indicated that the mice were not burdened, negating the need for an animal experiment proposal. Scientific assistants, the animal welfare officer of the Max Planck Institute Göttingen, and the veterinary institute Oldenburg of Niedersachsen for Consumer Protection and Food Safety (LAVES), which is the state office for animal welfare surveillance, verified this decision.

4.3. Study design

This research project included C57BL/6J mice, subdivided into male and female mice aged between 3 and 4 months. They were divided into three groups: Neuroligin 3 knockout (NL3-/y), Neuroligin 4 knockout (NL4-/y), and a control group of wild-types (WT). Initially, whole-body Dual X-ray Absorptiometry (DXA) was performed. After euthanasia, long bones (e.g., femur) were collected for further analysis. Histological evaluation using various staining methods, including immunohistochemistry, was conducted.

The first batch of mice bones was collected, and samples were embedded in February 2018. This batch had an unequal distribution of NL3-/y (n=5 (m=5)), NL4-/y (n=15 (m=8, f=7)), and WT (n=12 (m=8, f=4)) mice, totally 32 animals. To balance the groups, a second batch of 12 mice arrived in March 2019. The final group size included 44 mice, with the following distribution: NL3-/y (n=10 (m=8, f=2)), NL4-/y (n=19 (m=11, f=8)), and WT (n=15 (m=8, f=7)).

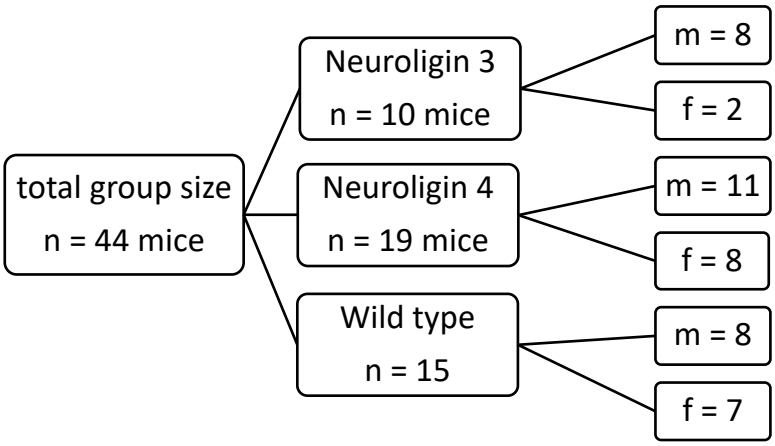

Figure 4: study design: one wild-type group (n=15) compared to two autistic mice models (NL3$^{-/y}$ n=10 and NL4$^{-/y}$ n=19)

4.4. Animal Housing

During their growth, skilled animal keepers cared for the mice, who were also under continuous veterinary observation. The mice were housed in small groups of two to four animals in the animal facilities at the MPI Göttingen. This team has extensive experience in breeding Neuroligin knockout mice since 2006. Both knockout and wild-type mice were fed standard complete feed from Sniff (42) ad libitum (= for free disposal) and always had access to fresh water.

4.5. Sample fixation

After receiving the mice from MPI Göttingen, bone harvesting was performed. The bones were immediately stored in saline-soaked gauzes at -20°C until further processing. This study focused on long bones, specifically the femoral bone, for analysis. The following chapters describe the processing of the histological samples.

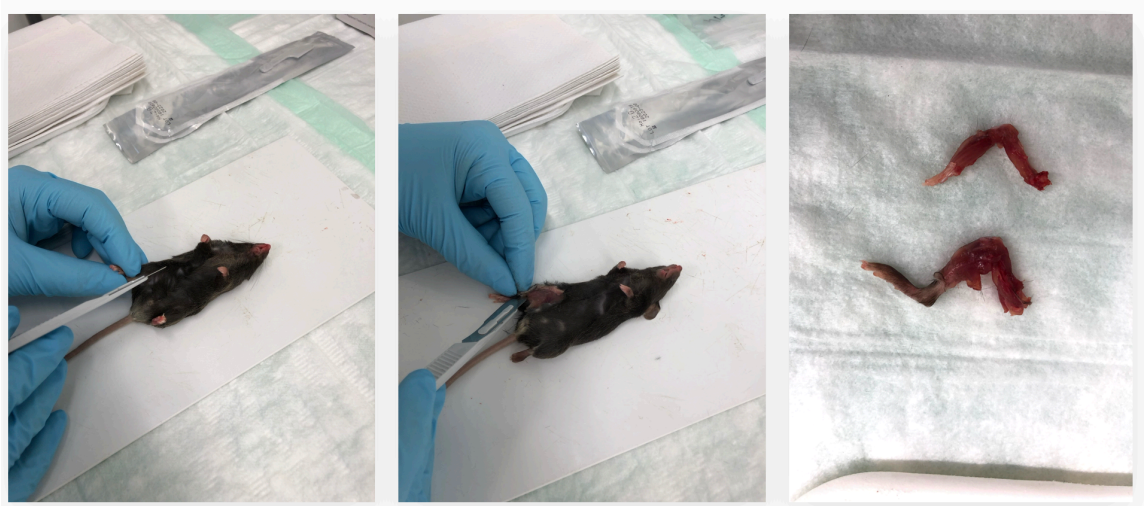

Figure 5: Bone harvesting: along the medial thigh, a longitudinal incision was made with a scalpel. Subsequently, the entire mouse leg was dissected free. The femur was separated from the skin and subcutaneous tissue, preserving the bone.

The bone samples were fixed in a 4% paraformaldehyde (PFA) solution for 48 hours at 4°C to initiate decalcification. To remove formalin residues, the samples were rinsed six times with sodium phosphate buffer. For careful decalcification, the bone samples were stored in embedding cassettes for approximately three weeks in a 1:2 mixture of 4% PFA and ethylenediaminetetraacetic acid (EDTA), with the solution being changed every 3 to 4 days. After three weeks, the samples were rinsed under running tap water for an hour, followed by dehydration and submersion in paraffin according to a fixed dehydration protocol outlined in Table 1.

Table 1: Dehydration procedure in the embedding (Leica EG1120, Leica Biosystems, Nussloch GmbH, Germany)

Step	Solution	Time in minutes	Repetition
1	Ethanol (70%)	60	1x
2	Ethanol (80%)	60	1x
3	Ethanol (96%)	120	2x
4	Ethanol (100%)	120	2x
5	Ethanol (100%)	180	1x
6	Xylene	60	2x
7	Paraffin	120	2x

Paraffin embedding and section slicing

The dehydrated samples were placed in preheated metal molds at 60°C to prevent the paraffin from solidifying instantly. The samples were carefully held with forceps on a heating plate while liquid paraffin was poured over them. Once the bones were fully covered with paraffin, the metal molds were placed on a cold plate at -10°C for 15 minutes to solidify the paraffin. After the paraffin fixation, the embedded samples were stored at room temperature.

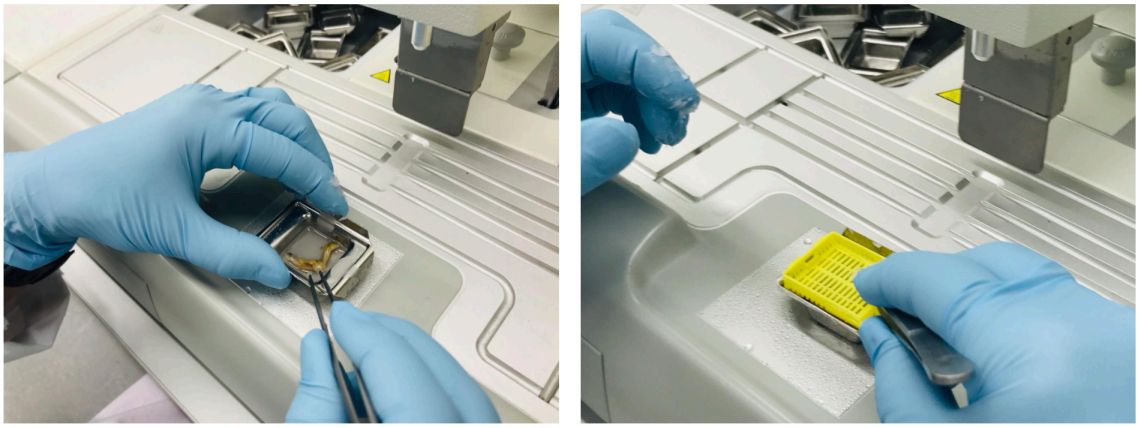

Figure 6: Paraffin embedding procedure of the collected femur bones from the mice: the dehydrated bone sample is placed in a metal mould and hold with a forceps, so the liquid paraffin could be gently poured over it.

After complete hardening, the paraffin cubes were cut into 5 µm thick sections using a motorized rotary microtome (Thermo/Microm HM 355S, Coolcutsystem, Thermo Scientific GmbH, Karlsruhe, Germany). These sections were placed in a warm water bath (40°C) to enable the slides to stretch. The final preparation step involved placing the sections on glass slides (Super Frost Plus®, R.Langenbrinck GmbH, Labor- und Medizintechnik, Emmendingen, Germany) and drying them overnight in an incubator at 37°C.

4.6. Dual Energy X-ray Absorptiometry (DXA)

Whole body DXA scans (GE Healthcare, Lunar Prodigy, Solingen, Germany, Scan mode: short, 1.8 µGy) were performed to measure bone mineral content (BMC), relative fat content (%), and bone mineral density (BMD) in one clinically relevant region of interest: the femur bone as described before (3,36). The DXA method is an established

technique for analyzing bone structure, commonly used in osteoporosis research to evaluate bone quality in specific regions of interest (46,47).

4.7. Histological staining

Histological staining of decalcified, paraffin-embedded sections helps visualize extracellular and cellular matrix organization (48,49). Focusing on bone, this study examines mineralization content closely. Multiple staining methods were used to image and differentiate cell types, enabling comparison across various groups to analyze metabolic processes.

All sections subjected to histological, enzymhistochemical, or immunohistochemical staining were further investigated under a light microscope, followed by histomorphometrical analysis.

4.7.1. Movat Pentachrome

Initially developed in 1955 by Henry Zoltan Movat, a Hungarian-Canadian pathologist, the Movat Pentachrome stain was designed to highlight tissue changes in cardiovascular tissue (50). The stain has been adapted for use on undecalcified bone sections. Following embedding in methyl methacrylate, this method produces favorable outcomes, showcasing vivid contrasts between mineralized and unmineralized regions in both cartilage and bone. It also enables differentiation of osteoblasts, osteoclasts, and various other cellular and tissue components (51). This staining technique is subdivided into five color sections, allowing detailed cellular evaluation. In histomorphometrical analysis, the different colors are classified as follows: osteoid (non-mineralized bone matrix) appears red, cartilage appears green, calcified bone appears yellow, and fibrous/connective tissue appears grey.

Table 2: Staining protocol for Movat Pentachrome

Step	Solution	Repetition	Time (min)
1	Deparaffinize in Xylene	2x	5
2	Descending alcohol concentration (100%, 96%, 70%)	1x	2
3	Rinse in distilling water (briefly)		
4	Encircling the section with fat marker (‘pap pen’)		
5	Alcian blue stain	1x	10

6	Rinse in tap water	1x	5
7	Alkaline ethanol (EtOH)	1x	60
8	Rinse in tap water	1x	10
9	Rinse in distilling water (briefly)		
10	Weigert's Iron Hematoxylin stain (horizontal)	1x	10
11	Rinse in distilling water (briefly)		
12	Rinse in tap water	1x	15
13	Brillian Crocein – Acid Fuchsine stain	1x	12,5
14	Acetic acid 0,5% (briefly)		
15	Phosphotungstic acid 5%	1x	20
16	Acetic acid 0,5% (swing)	1x	2
17	Ethanol 100%	3x	5
18	Saffron du gatinais	1x	60
19	Ethanol 100%	3x	2
20	Xylene	2x	5
21	Embedding in Vitroclut		

4.8. Enzyme histochemical staining's

Various enzymes are located on cells (52). To make them optically visible, a colorless substrate is added to the tissue. This substrate is catalyzed by the enzyme on the cell/tissue surface, resulting in a colored conjugate. This method facilitates the localization and quantification of specific enzymes in tissue specimens. Optimally, staining is performed on fresh tissue specimens. After fixation, assessing enzyme activity is not possible, but imaging cells covered with a specific enzyme is still feasible (52).

4.8.1. Tartrate-Resistant Acid Phosphatase (TRAP)

Tartrate-Resistant Acid Phosphatase (TRAP) is expressed in the bone and the immune system and can be found on many cell types, including macrophages, dendritic cells, and osteoclasts (53). In bone metabolism, osteoclasts are the only cells capable of bone resorption (54). To evaluate and estimate bone depletion, the typical TRAP expression of osteoclasts is utilized. TRAP is a sensitive marker for osteoclastic activity (55). Immunohistochemically stained multinuclear cells, attached to the bone surface with a ruffled border, were counted and measured in length. This staining method highlights osteoclastic activity in red, allowing for quantification and measurement of their length. These parameters enable the assessment of osteoclastic activity.

TRAP Solution:

Substrate 1: Dissolve 35 mg Naphthol-AS-TR-Phosphat in 125 µl N-N-Dimethylformamid

Substrate 2: 1. Solve 57,5 mg di-Natriumtartrat-Dihydrat in 1ml Sodium acetate buffer
2. 35 mg of Echtrotsalz in 1ml Sodium acetate buffer (Eppendorf tube)

Substrate 1 is pipetted in Substrate 2. The solution shows a slightly red colour.

Table 3: Staining protocol for TRAP

Step	Solution	Repetitions	Time (min)
1	Deparaffinize in Xylene	2x	5
2	Descending alcohol concentration (100%, 96%, 70%)	1x	5
3	Rinse in distilled water	2x	5
4	Rise with 0,1 M sodium acetate buffer (pH 4,9 – 5,2)	1x	10
5	Encircling the section with fat marker (‘pap pen’)		
6	Staining with TRAP-solution in humidity chamber (37°C)	1x	30
7	Rinse in distilled water	3x	5
8	Counterstaining in hematoxylin	1x	1
9	Rinse in distilled water	1x	1
10	Rinse in tap water	1x	10
11	Rinse in distilled water	1x	5
12	Embedding in Vitro clut		

4.9. Immunohistochemical staining’s

Immunohistochemistry (IHC) staining helps analyze the activity, distribution, and arrangement of different cell types. By detecting antigens on cell surfaces with specific antibodies, different epitopes can be visualized, presenting surface proteins characteristic of particular cell types or the extracellular matrix (17). This technique enables researchers and clinicians to identify and localize certain cell types, pathological alterations, or biomarkers within tissue specimens. The antigen-antibody complex activates an enzyme-labeled specific color reaction, allowing conclusions to be drawn about metabolism, particularly when combined with previous histological stainings (56).

4.9.1. Osteocalcin

To investigate osteoblastic activity, osteocalcin (OCN) detection was carried out. This cell surface marker is found on odontoblasts in teeth and osteoblasts in bone. Previous studies demonstrate that the non-collagenous protein OCN impacts bone formation, matrix organization, and osteoblastic activity (57,58). Compared to TRAP staining, which evaluates osteoclast activity, this study aims to elaborate on osteoblast activity in the above-named models.

4.9.2. CD68

CD68, or Macrosialin, is an immunohistochemical marker located intracellularly and on the surface of monocytes, macrophages, dendritic cells, granulocytes, T- and B-lymphocytes. The exact function of CD68, likely as a scavenger receptor, needs further confirmation (17,59).

In this study, this marker is used to identify all macrophages, serving as a foundation for subsequent staining, where the division into M1 and M2 stage macrophages will be made.

4.9.3. CD80

CD80, commonly known as B7-1, is a cell surface molecule expressed especially on dendritic cells, activated B-cells, and macrophages. Its role is co-stimulation for T-lymphocyte activation (17,60).

For differentiating M1 and M2 macrophages, CD80 is the marker for M1 macrophages, which primarily evoke a pro-inflammatory reaction by initiating regenerative processes (5).

4.9.4. CD206

CD206, or macrophage Mannose receptor, is predominantly expressed on the surface of alternatively activated macrophages. These M2 stage macrophages, unlike their M1 counterparts, are characterized by their anti-inflammatory effect. This makes M2 macrophages essential for tissue remodeling, resolving inflammation, inducing immune tolerance, and protecting against excessive inflammatory responses (5).

Table 4: General Protocol for Immunohistochemical Staining

Step	Solution	Repetitions	Time (min)
1	Deparaffinize in Xylene	2x	5
2	Wash in technical acetone	1x	10
3	Mix technical acetone + washing buffer 1:1 concentration	1x	10
4	Rehydrate the slides in washing buffer	2x	10
5	Antigen retrieval using citrate buffer solution (pH=6)	1x	60
6	Wash the slides in washing buffer at room temperature	2x	5
7	Mark around the section using fat marker (‘pap pen’)		
8	Bloxal blocking to inhibit endogenous peroxidase	1x	10
9	Wash the slides in washing buffer at room temperature	1x	5
10	Add one drop of universal serum in 5 ml of TBS		
11	Incubate slides at room temperature	1x	20
12	Incubate with primary antibody at 4°C (overnight)		
13	Wash in washing buffer	2x	5
14	Prepare secondary antibody by adding a drop of universal serum and a drop of biotinylated universal antibody in 2,5 ml of TBS		
15	Incubate with secondary antibody at room temperature	1x	30
16	Prepare ABC-AP complex (30 minutes before use): add 25 µl Reagent A and 25 µl Reagent B in 2500 µl of TBS		
17	Rinse in washing buffer	2x	5
18	Incubate in ABC-AP complex at room temperature	1x	30
19	Rinse in distilled water	1x	5
20	Mix AP substrate mix by adding all three reagents (2 drops each) in 5 ml of 150 mM Tris-HCl buffer (pH 8,3)		
21	Incubate until red color is detected		
22	Rinse in distilled water to stop the reaction	2x	5

23	Counter stain with methyl green (incubate at 60°C)	1x	5
24	Washing and rinse the slides in distilled water	1x	1
25	Add 50 µl glacial acetic acid in 100 ml acetone, dip the slides 5-10 times in the solution		
26	Dip the slides in Ethanol (96%, 100%; 5 times each)		
27	Dry the slides in the incubator at 60°C	1x	30
28	Embedding in Vitro clut		

4.10. Image Analysis

The image capturing was performed with a light microscope (Leica Microscope, Leica DM5500 photomicroscope, DFC 7000 camera, LASX software version 3.0; Leica Microsystem Ltd., Wetzlar, Germany). The immunohistochemical staining's to mark Osteocalcin, CD68, CD80 and CD206 were imaged using 10X magnification. The Movat Pentachrome and TRAP staining were imaged with 40X magnification, the Movat Pentachrome additionally in 5X magnification to get overview visualization.

To evaluate the histomorphometry, ImageJ software (version 1.51n, National Institute of Health, Bethesda, MD, USA) was utilized. In this, an automated plugin (48) based on Trainable Weka Segmentation (version 3.2.13) plugin (61) was used to quantify different parameters (such as bone area, CD80 positive area) from histological stains.

4.11. Statistical Analysis

For statistical analysis, the SPSS program (IBM SPSS Statistical Package 24.0, IBM Corporation, Armonk, New York, USA) was used. First, the dispersion of data regarding normal distribution was examined using QQ-plots, revealing that none of the results were normally distributed. Based on the data type (non-parametric), appropriate statistical tests were carried out to evaluate significant differences. The significance level was set at $\alpha = 0.05$, with a p-value <0.05 considered significant.

Within the scope of the target parameters, the two knockout groups were compared with the wild-type group. Descriptive statistics were conducted, and bar graphs were analyzed, represented as Mean ± Standard Error of the Mean (SEM). The standard deviation (SD) was also included.

The main target parameters of the study include:

1. BMD, BMC, and %Fat using radiological DXA method
2. Histomorphometric analysis of bone structure using Movat Pentachrome staining
3. Immunohistochemical measurement of osteoclast quantity and activity using TRAP staining
4. Immunohistochemical measurement of osteoblast quantity and activity using Osteocalcin staining
5. Immunohistochemical measurement of macrophage quantity and activity using CD68, CD80, and CD206 staining

5. Results

The initial step of this project involved investigating the percentage distribution in the three groups using whole-body DXA.

Regarding Bone Mineral Content (BMC), the NL4 knockout group exhibited a slightly lower mineral content (0.29 ± 0.08, p>0.05) compared to both the NL3 knockout group (0.36 ± 0.14, p>0.05) and the wild-type group (0.36 ± 0.05, p>0.05) (Figure 7).

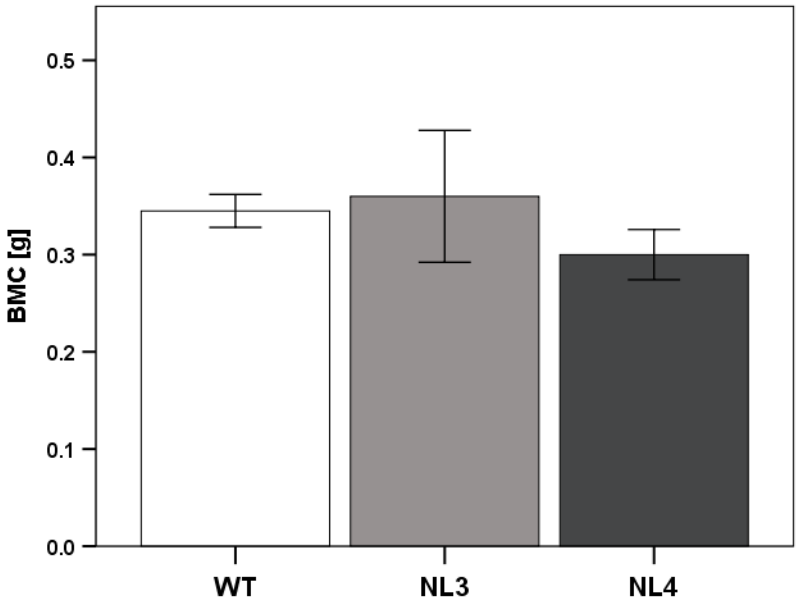

Figure 7: Bone Mineral Content (BMC, in g) in dual energy X-ray absorptiometry: NL3 and NL4 knockout mice did not exhibit a statistically significant difference in BMC compared to WT controls. (n = 10 (NL3), n = 19 (NL4), n = 15 (WT)).

For Bone Mineral Density (BMD), although no significant differences were observed among the groups, the BMD in the NL4 knockout group (0.08 ± 0.01, p>0.05) was marginally higher than that in the wild-type group (0.07 ± 0.01, p>0.05) and the NL3 knockout group (0.07 ± 0.01, p>0.05) (Figure 8).

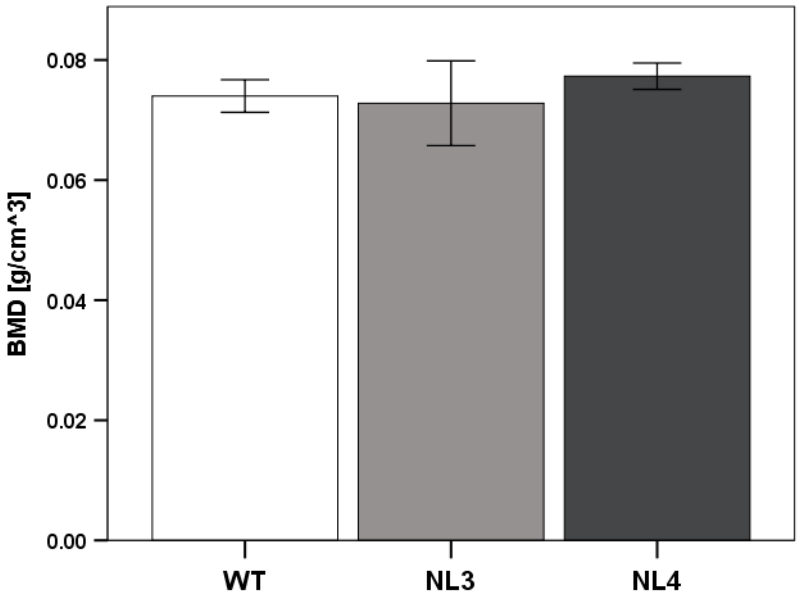

Figure 8: Bone Mass Density (BMD, in g/cm^3) in dual energy X-ray absorptiometry: no significant differences in BMD in the knockout groups NL3 and NL4 compared to the WT group was elucidated. (n = 10 (NL3), n = 19 (NL4), n = 15 (WT)).

The percentage of fat in the different groups showed significant differences. The NL4 knockout group had a significantly lower fat percentage (9.43% ± 5.99%, p>0.05) compared to the wild-type group (19.09% ± 5.19%, p=0.01). The NL3 knockout group (14.40% ± 7.04%, p>0.05) showed no significant differences compared to either the wild-type or the NL4 knockout group (Figure 9).

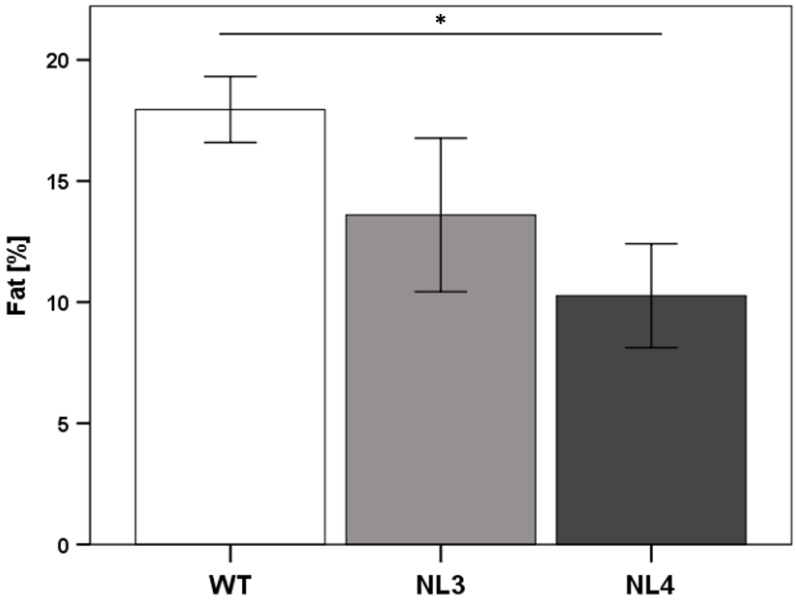

Figure 9: Fat in % in dual energy X-ray absorptiometry: %Fat in NL4 knockout mice was seen compared to the wild-type mice. No significant differences in between NL3 knockout mice and wild-type mice were seen. (n = 10 (NL3), n = 19 (NL4), n = 15 (WT)).

Movat Pentachrome Staining

In the wild-type group, the metaphyseal area/growth plate appeared as expected (Figure 10, A). Osteocytes embedded in calcified bone were clearly depicted in all groups (Figure 13, A3-C3).

In the Neuroligin 3 knockout group, a normal metaphyseal area/growth plate was observed (Figure 10, B). A high percentage of adipose tissue was identified at the periosteum (Figure 12, B2). No significant differences in the count of monocytes were seen, the osteocyte morphology was normal (Figure 13, B3). The chondrocytes exhibited a reduced capacity for proliferation.

In the Neuroligin 4 knockout group, fewer chondrocytes were observed, and the mineralized part of the growth plate was smaller than in the Neuroligin 3 and wild-type groups (Figure 10, C). There were also fewer proliferative chondrocytes. Generally, fewer monocytes were identified in the bone marrow (Figure 12, C2), and the osteocytes were surrounded by an unmineralized area.

Compared to the wild-type group, the NL3 and NL4 knockout mice showed the presence of partially mineralized fibrous tissue (Figure 11, B1-C1). In the knockout groups, an increased number of immune cells, such as monocytes, were seen in the bone marrow region.

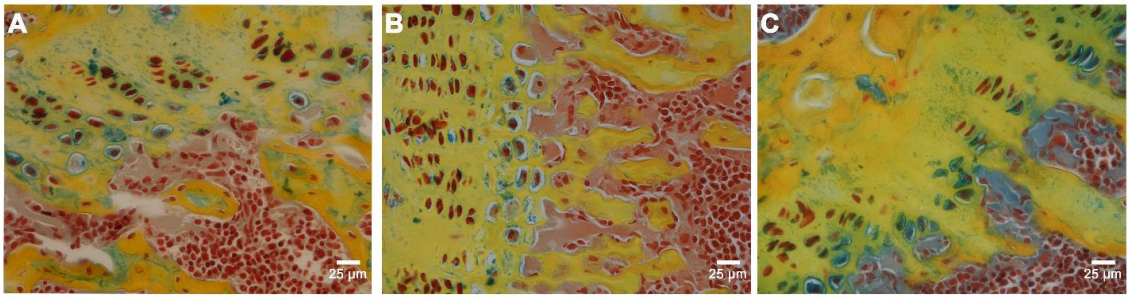

Figure 10: Movat Pentachrome Staining of the growth plate (A = wild-type group, B = Neuroligin 3 knockout, C = Neuroligin 4 knockout; osteoid (red), cartilage (green), calcified bone (yellow), fibrous tissue (gray), background (black/white). In the wild-type group, the growth plate appears as expected with abundant proliferative chondrocytes and surrounding calcification zone with osteoid as well as already mineralized bone. In the NL3 and NL4 groups, numerous chondrocytes were also observed.

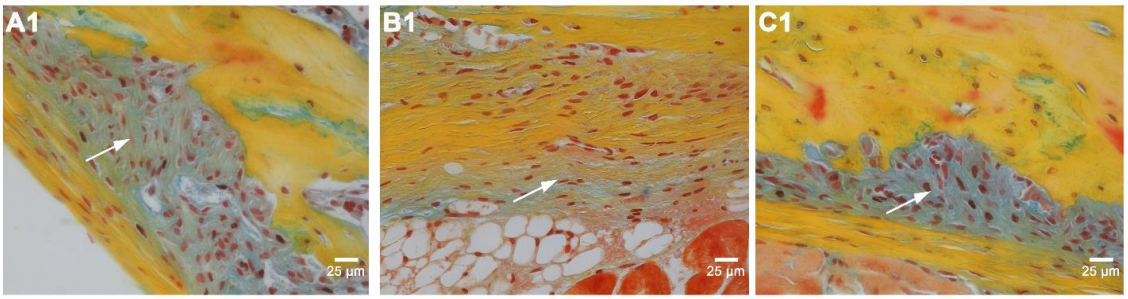

Figure 11: Movat Pentachrome Staining of the periost (A1 = wild-type group, B1 = Neuroligin 3 knockout, C1 = Neuroligin 4 knockout; osteoid (red), cartilage (green), calcified bone (yellow), fibrous tissue (gray), background (black/white). Compared to the wild-type group, the NL3 and NL4 knockout mice shows the presence of partially mineralized fibrous tissue (marked with arrows). In the NL3 knockout group, in the vicinity of the periosteum, plentiful adipose tissue cells could be shown.

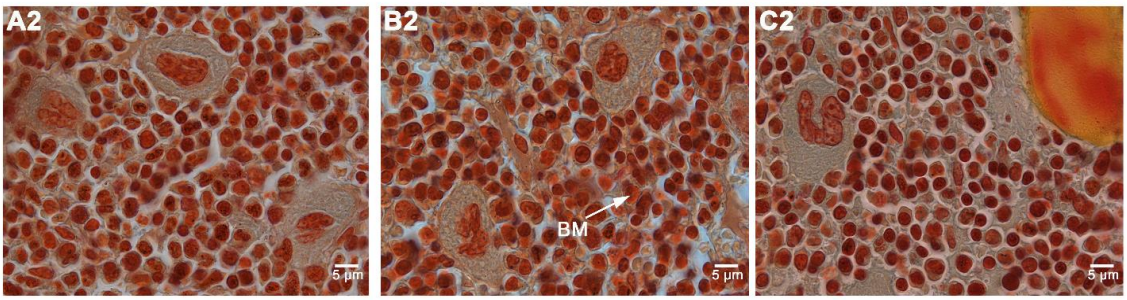

Figure 12: Movat Pentachrome Staining of the bone marrow/fat (A2 = wild-type group, B2 = Neuroligin 3 knockout, C2 = Neuroligin 4 knockout; osteoid (red), cartilage (green), calcified bone (yellow), fibrous tissue (gray), background (black/white), BM = bone marrow. In the knockout groups an increased number of immune cells, such as monocytes, were seen in the bone marrow region.

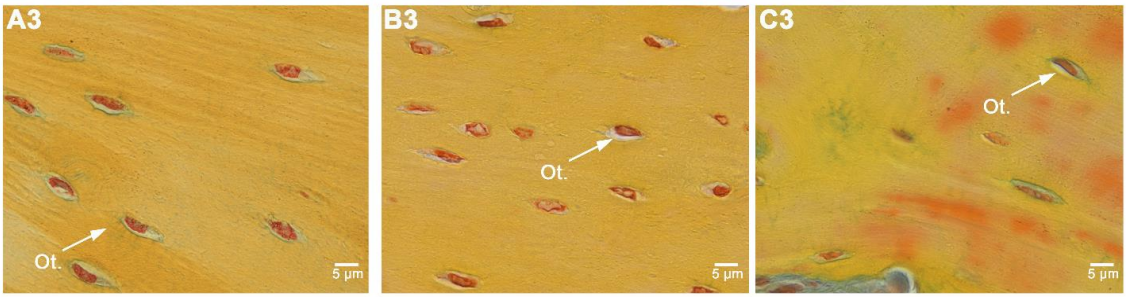

Figure 13: Movat Pentachrome Staining of the corticalis (A3 = wild-type group, B3 = Neuroligin 3 knockout, C3 = Neuroligin 4 knockout; osteoid (red), cartilage (green), calcified bone (yellow), fibrous tissue (gray), background (black/white), ot. = osteocytes. Osteocytes could clearly depicted in all groups, embedded in calcified bone.

TRAP and Osteocalcin Staining

TRAP staining was used to highlight osteoclasts by examining the positively labeled regions across the entire bone surface (Figure 14). When comparing the number of osteoclasts among the different groups, the Neuroligin 3 knockout group exhibited a non-significant but slightly higher number of osteoclasts compared to both the wild-type and

Neuroligin 4 knockout groups. The wild-type group and the Neuroligin 4 knockout group had nearly the same number of osteoclastic cells (Figure 15).

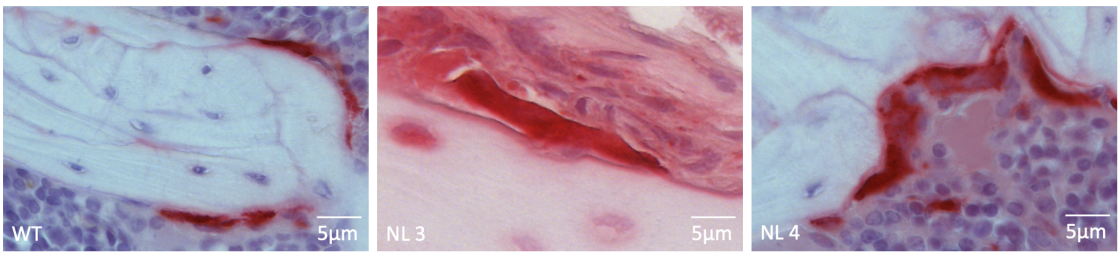

Figure 14: Osteoclasts marked by using TRAP Immunohistochemical Staining: The length of the surface side is measured from the osteoclasts to assess the osteoclastic activity.

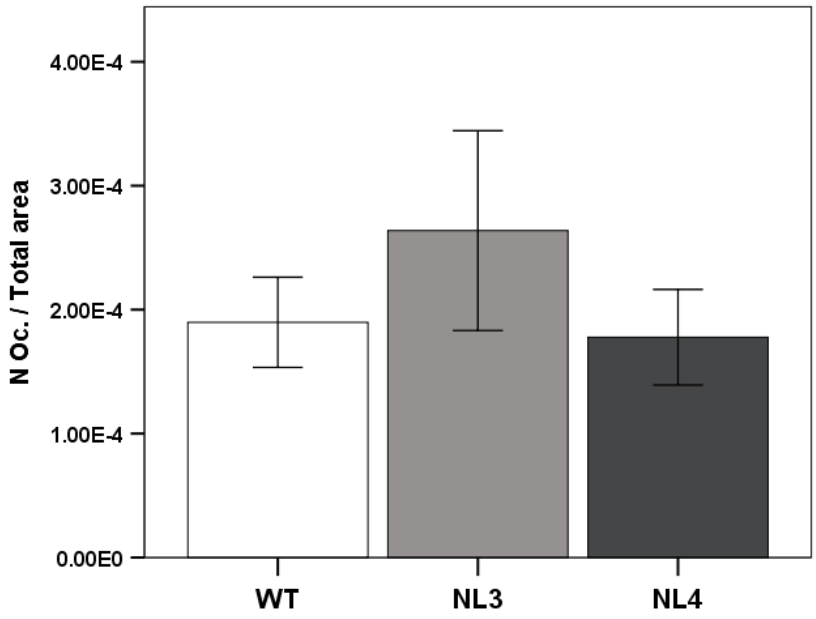

Figure 15: Number of osteoclasts / Total area: In the NL3 group, a marginal increase in the number of osteoclasts per total area was noted compared to both the NL4 knockout and wild-type group, although this disparity was not statistically significant. (n = 10 (NL3), n = 19 (NL4), n = 15 (WT))

By analyzing the osteoclastic activity per total area, a clearly increased activity was observed in the Neuroligin 3 knockout group, although the distribution breadth in this group was twice as great as in the other two groups, wild-type and Neuroligin 4 knockout.

Comparing the wild-type group with the Neuroligin 4 knockout group, a slightly increased osteoclastic activity was observed in the wild-type group (Figure 17).

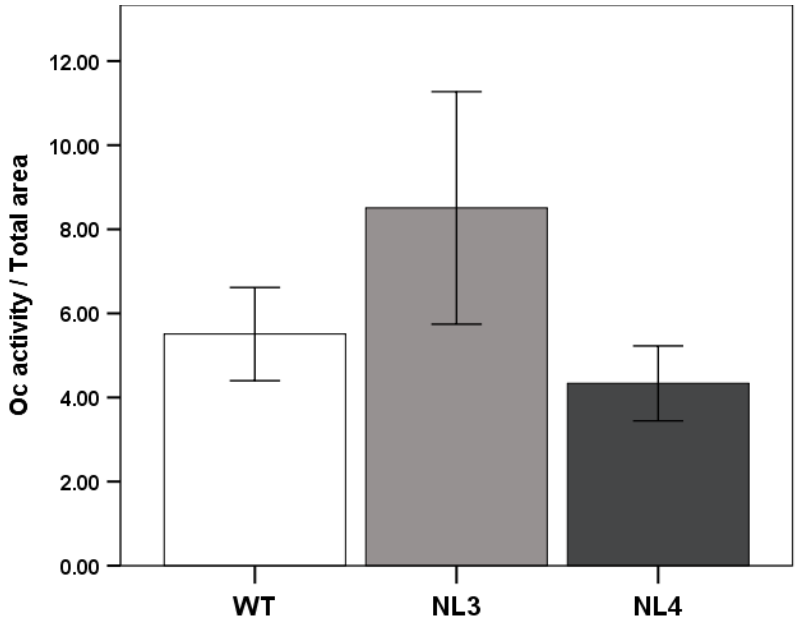

Figure 16: Osteoclastic activity per total area: a clearly increased activity of osteoclasts was elucidated in the NL3 knockout mice compared to the NL4 knockout and WT mice (n = 10 (NL3), n = 19 (NL4), n = 15 (WT)).

Osteoblasts were visualized in the Osteocalcin (OCN) staining. The wild-type and Neuroligin 4 knockout groups showed a significantly reduced percentage of OCN-positive areas compared to the Neuroligin 3 knockout group. The wild-type group exhibited a slightly higher proportion of osteoblasts in the examined regions compared to the Neuroligin 4 group (Figure 17).

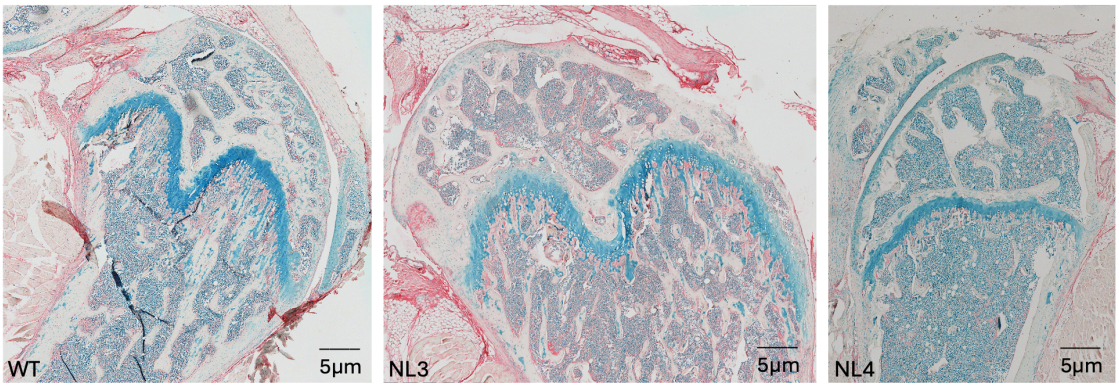

Figure 17: Osteoblasts marked by using Osteocalcin Immunohistochemical Staining.

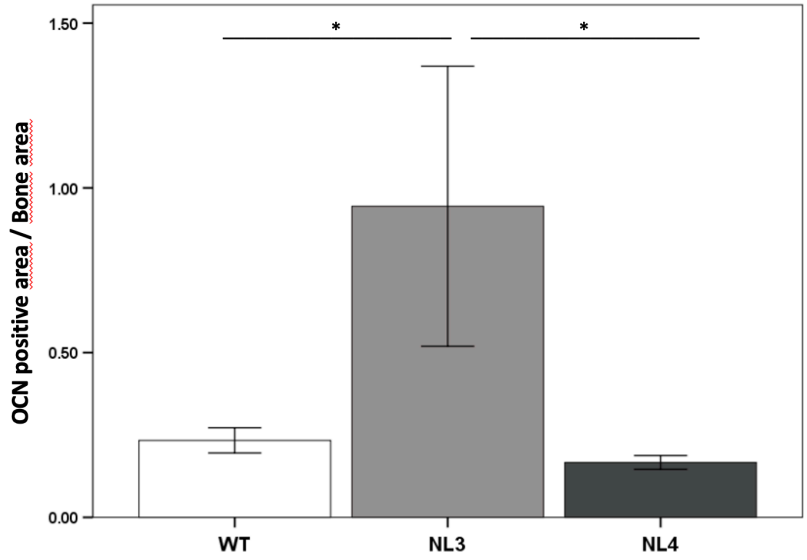

Figure 18: Osteocalcin positive area / Bone area: WT and NL4 groups show a significantly reduced percentage of OCN positive areas compared to the NL3 knockout group. (n = 10 (NL3), n = 19 (NL4), n = 15 (WT)).

Immunohistochemical Staining of Macrophages

Using immunohistochemical stainings, a histological analysis was conducted to characterize and identify the different activated macrophages (M1 and M2). M1 macrophages were characterized with surface marker CD80, and M2 macrophages with surface marker CD206. Both types were visualized using the CD68 marker.

Regarding the positively marked bone areas colonized with macrophages (marked with CD68+), no extreme differences were observed between the wild-type and knockout groups. However, there was a slightly increased percentage of positively marked bone

areas in the Neuroligin 3 and 4 knockout groups compared to the wild-type group (Figures 18 and 19).

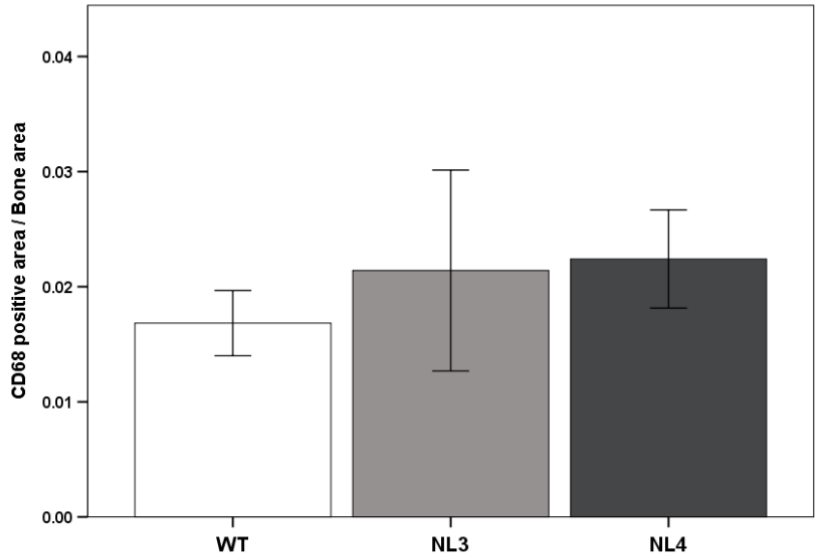

Figure 19: CD68 positive area / bone area (CD68 as a marker for all macrophages): In both, the NL3 and NL4 knockout groups, a slight increase is observed in the proportion of bone areas positively marked, relative to the wild-type group. (n = 10 (NL3), n = 19 (NL4), n = 15 (WT)).

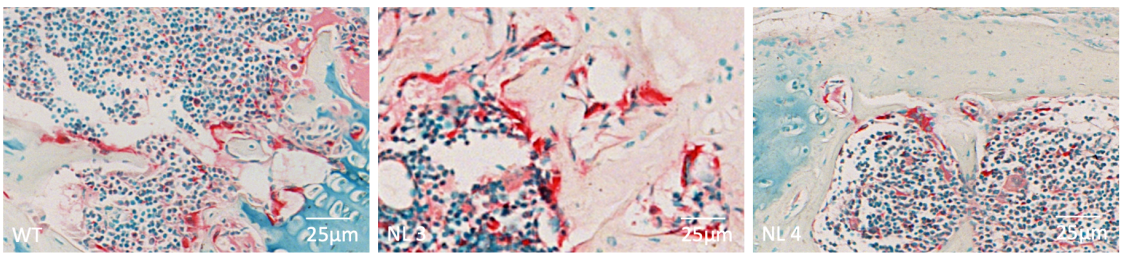

Figure 20: CD68 marking both M1 and M2 macrophages

By using the CD80 marker, M1 macrophages were represented. The wild-type group exhibited a noticeably lower average percentage of M1 macrophages compared to both the Neuroligin 3 and Neuroligin 4 knockout groups. However, the distribution range within all groups was considerable, and no statistically significant differences were observed (Figures 20 and 21).

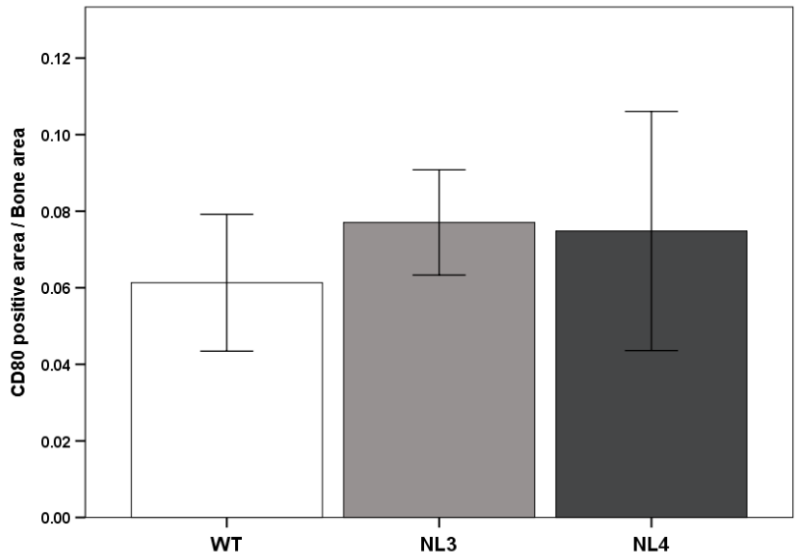

Figure 21: CD80 positive area / bone area (CD80 as a marker for M1 macrophages): The percentage of M1 macrophages in the WT group is clearly lower average compared to the NL3 and NL4 knockout groups, nevertheless the range in all groups is large. (n = 10 (NL3), n = 19 (NL4), n = 15 (WT)).

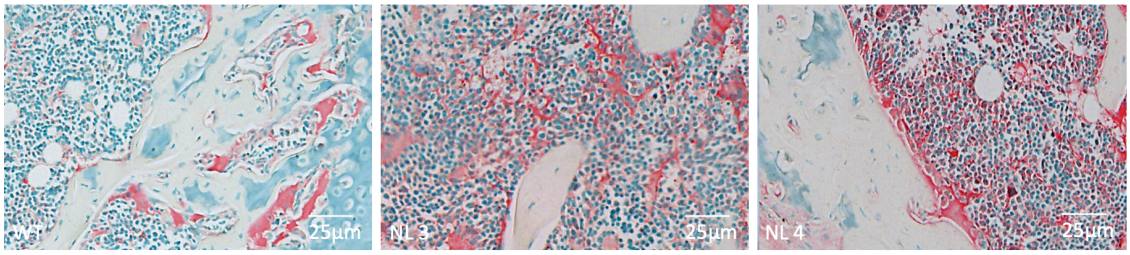

Figure 22: CD80 marker to highlight M1 macrophages

To quantitatively assess M2 macrophages, immunohistochemical staining for the surface receptor for Mannose (CD206) was performed. This experiment revealed a significantly higher percentage of M2 macrophages in the Neuroligin 3 group compared to the wild-type and Neuroligin 4 knockout groups. The Neuroligin 4 knockout group exhibited the lowest CD206-positive area per bone area compared to the wild-type and Neuroligin 3 knockout groups (Figures 22 and 23).

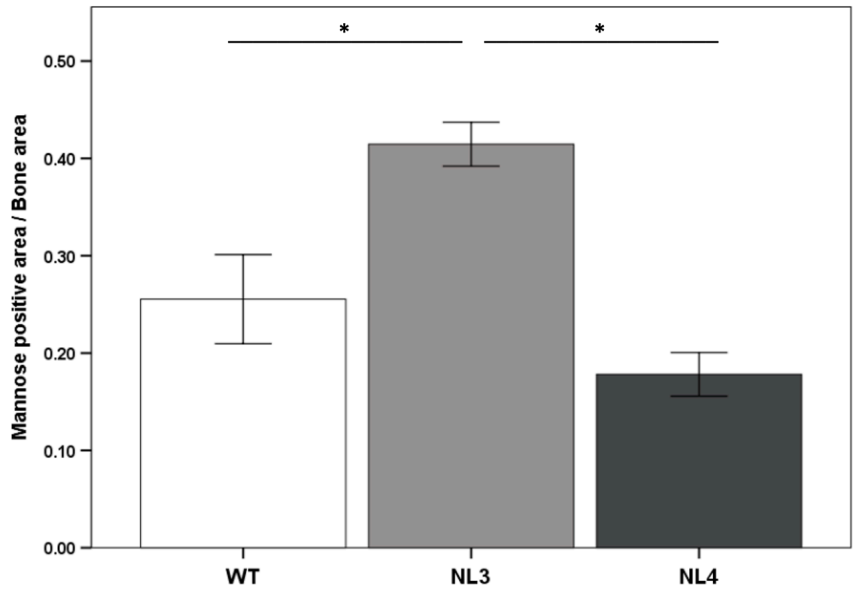

Figure 23: CD206/Mannose positive area / bone area (CD206 as a marker for M2 macrophages): in the NL3 knockout mice a significant higher percentage of M2 macrophages were seen compared to both the NL4 knockout and wild-type groups. (n = 10 (NL3), n = 19 (NL4), n = 15 (WT)).

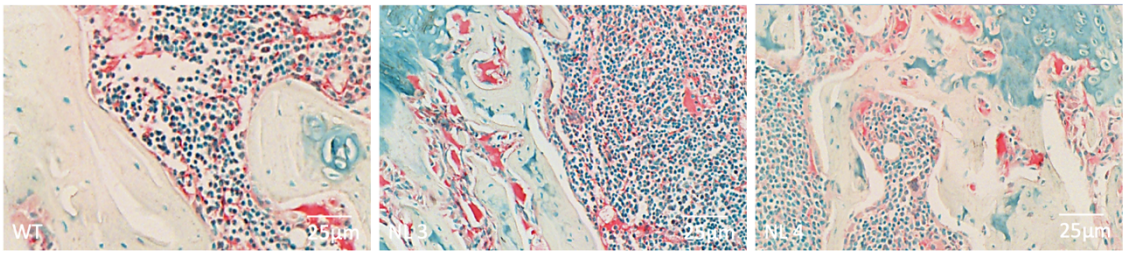

Figure 24: CD206 marker to highlight M2 macrophages

6. Discussion

This thesis, aimed to uncover distinctions in cellular bone metabolism and histomorphometry between the Neuroligin 3 (NL3) and Neuroligin 4 (NL4) knockout groups and the wild-type group. No significant differences were observed between male and female experimental animals; therefore, the focus was on the overall cohort, subdivided into the experimental groups: wild-type, Neuroligin 3, and Neuroligin 4.
Additionally, immunohistochemical investigations were conducted to shed light on the influence of macrophages in this model. Radiological examinations did not reveal significant differences among the groups. Histomorphometry revealed alterations in bone structure, such as a modified arrangement of the growth plate. Immunohistochemistry demonstrated varying distribution of macrophages between M1 and M2 phenotypes.

Several studies have highlighted orthopedic consequences or disorders in other monogenetic neurodevelopmental conditions, such as Rett Syndrome (61). This neurological disorder, attributed to a mutation in the MECP2 gene, correlates with orthopedic complications, including scoliosis, osteopenia, and an increased risk of fractures (62).

ASD has a relevant impact on the qualitative and quantitative bone metabolism

Reflecting on the objectives outlined for this study, several key points can be expounded upon. The primary aim was to demonstrate the significant influence of ASD-associated knockout of Neuroligin 3 and 4 on bone metabolism. Therefore, radiological and histological analyses were employed to investigate disparities between a group of wild-type mice and two knockout groups (NL3 and NL4). Previous literature has detailed impaired bone microarchitecture parameters, with numerous recent publications reporting decreased BMD in adolescent boys affected by ASD (2,36). However, our dual X-ray absorptiometry did not reveal these reported differences; only slight, non-significant disparities were observed. Rostami et al. (2021) similarly reported a decrease in BMC in children with ASD (35). The reduced BMD reported in the literature was not in agreement with our investigations. Only minimal differences, with a trend towards lower BMD in the NL3 knockout group and a trend towards higher BMD in the NL4 knockout group, were observed between the wild-type group and both knockout groups. However, there appears to be a reduction in the percentage of fat in bone in the Neuroligin 4 knockout group compared to both the wild-type and Neuroligin 3 groups. Fat has lower stability and strength compared to calcified bone, potentially resulting in inferior bone structure (63).

Histomorphological Findings

In the histomorphological analysis using Movat Pentachrome Staining, the growth plate appeared smaller in the NL4 knockout group compared to the other two groups. This observation suggests a potentially significant influence of NL4 knockout on bone growth. Moreover, the NL3 knockout group exhibited elevated osteoclastic activity and a higher quantity of TRAP-positive osteoclasts, as well as an increased presence of Osteocalcin-positive labeled osteoblasts. These findings suggest an augmented rate of bone resorption and enhanced bone formation within this experimental group. A four to five times higher percentage of osteoblasts was observed in the NL3 knockout group compared to the NL4 knockout and wild-type groups, indicating a significant impact of NL3 and NL4 knockouts on bone metabolism.

Cellular Distribution and Bone Remodeling

In the Movat Pentachrome Staining, discrepancies and cellular distributions were illustrated in the knockout groups compared to the wild-type group. Proliferative chondrocytes were observed in all groups surrounding the metaphyseal area near the growth plate, and numerous embedded osteocytes were depicted in all groups, indicating fundamentally physiological bone metabolism. In the NL3 and NL4 knockout groups, partially mineralized fibrous tissue was evident. Fibrous tissue and cartilage constitute the soft callus in fracture healing, which is typically replaced by hard callus over time in normal fracture healing (5). Fewer chondrocytes and mineralized tissue were seen in the NL4 group compared to the NL3 and wild-type groups. Furthermore, a greater presence of immune cells was noted in the knockout mouse groups.

In other animal experimental studies, it has been demonstrated that neurological developmental disorders such as Tatton-Brown-Rahman Syndrome, which is associated with a genetic mutation in the DNMT3A gene, exhibit poorer bone quality. In addition to cortical bone thinning, indicative of mechanical impairment, larger bone marrow adipocytes have also been described (64). In our study, increased fat deposition near the periosteum was similarly demonstrated.

A reduced network of canaliculi in osteocytes was observed in the NL3 and NL4 knockout groups. Parallels have been described between a diminished network of osteocyte canaliculi and deteriorated bone quality. Research on various bone disorders, including osteoporosis in the elderly, has focused on degenerative changes in osteocytes and their lacuna-canalicular system. In osteoporotic bone, there is an imbalance between continuous bone resorption by osteoclasts and decreased bone formation by

osteoblasts. This imbalance increases the risk of fractures (65). The role of the osteocyte network and its influencing factors, potentially including interactions with immune cells such as macrophages, are not yet fully understood. For instance, osteocyte apoptosis has been described as an enhancing factor of bone resorption, releasing intracellular factors that include immunomodulatory molecules (66).

Impact of Neuroligin Knockouts on Bone Metabolism

The study revealed an impact of NL3 and NL4 knockouts on osteoclast activity, with increased activity observed in the NL3 group. Additionally, decreased bone-forming osteoblastic activity was demonstrated in the NL4 knockout group, while the NL3 group showed increased expression. This imbalance could suggest an enhanced bone demineralization in the NL4 knockout group.

An impaired bone structure was seen on cellular and metabolic level in NL3 and NL4 knockout mice

The second objective aimed to elucidate cellular and metabolic discrepancies in the examined models and demonstrate that these differences culminate in impaired bone structure. The Movat Pentachrome staining revealed multiple divergences upon comparing the two knockout groups to the wild-type group. The growth plate in the NL3 knockout group exhibited similarity to the wild-type group, while the NL4 knockout group displayed evident narrowing of the same structure. Histomorphological examination in Movat Pentachrome staining revealed an increased percentage of adipose tissue at the periosteum in the NL3 group compared to the wild-type group, whereas significantly less fat was observed in the NL4 group. Adipose tissue inherently offers less stability compared to calcified bone (67). Additionally, fewer monocytes were evident in the bone marrow of the NL4 group compared to the other two groups, despite the overall detection of immune cells in the bone via immunohistochemical stains.

A notably increased presence of macrophages in stage M1 relative to those in stage M2 was observed in the NL4 knockout group, suggesting a prevailing pro-inflammatory metabolic state. In osteoclast-detecting stains, a reduced quantity of osteoclasts was observed in the NL3 knockout group, whereas a higher number was detected in the NL4 knockout group. These knockout conditions may induce pertinent changes in bone structure due to an altered bone remodeling rate. Continuous and balanced homeostasis is vital for the functional integrity and strength of bone mass (58).

Immunological Influence on Bone Metabolism

The NL3 knockout group in the TRAP and Osteocalcin staining revealed a markedly elevated count of both osteoblasts and osteoclasts compared to the other groups, indicating distinctions at both the metabolic and cellular levels. An increased number of bone-forming and bone-resorbing cells in the NL3 knockout group compared to the wild-type group may indicate an accelerated bone metabolism. The investigations of M1 and M2 macrophages showed a significantly increased proportion of M2 macrophages as well as an increased proportion of M1 macrophages in the NL3 group compared to the wild-type group, suggesting an immunological influence on bone metabolism. In both the NL3 and NL4 groups, an increased presence of macrophages was observed in the CD68 staining compared to the wild-type group. The influence of immune cells, such as macrophages, on osteoblast and osteoclast activity can have a relevant impact on bone metabolism depending on their polarization (68).

Macrophages show different appearance in NL3 and NL4 knockout and wild-type group

The final objective focused on elucidating the role of macrophages. As integral components of the immune system, their impact on bone metabolism and their altered presence in the knockout models compared to the wild-type model were investigated. A reduced count of monocytes was observed in the NL4 knockout group in histomorphological analysis compared to the other groups. Immunohistochemical staining with the CD68 marker revealed a greater abundance of marked macrophages in the knockout groups than in the wild-type group. Further staining was conducted to subdivide the macrophages into M1 and M2 stages. In the CD80 marker staining, M1 macrophages were more prevalent in the NL3 and NL4 knockout groups compared to the wild-type group. However, on average, slightly more positively marked areas or macrophages were observed in the NL3 knockout group compared to the NL4 knockout group.

M1/M2 Macrophage Ratio

Upon assessing the ratio of M2 to M1 macrophages, a higher prevalence of positively labeled M2 macrophages was observed in all groups. An imbalance between M1 and M2 macrophages in bone can have significant implications for bone health and homeostasis. M1 and M2 macrophages represent two distinct phenotypes with different functions and effects on bone metabolism (69). A significant difference was observed between the NL3 knockout group and the NL4 knockout group, with a threefold higher proportion of positively marked areas of macrophages in the former and a twofold higher

proportion in the wild-type group. While M1 macrophages typically act pro-inflammatory, M2 macrophages are anti-inflammatory and have tissue repair and remodeling functions. An increase in M1 macrophages in bone is often associated with bone loss/increased bone resorption, while an increase in M2 macrophages is generally associated with decreased bone resorption and increased bone formation. An imbalance in the M1/M2 ratio is associated with conditions such as osteoporosis (20) or pseudarthrosis (70). Therapeutic approaches that may alter macrophage polarization and thus represent an immunomodulatory treatment approach have been explored (20). Chronic inflammation is suggested when there is an uneven distribution of M1 and M2 macrophages, as observed in this study. Furthermore, an upregulation of macrophage activity in pseudarthrosis was also noted.

Role of Macrophages in Bone Metabolism

This immunohistochemistry study attempted to elucidate the role of macrophages in bone metabolism. Macrophages are an extremely adaptable cell population (5). Preliminary studies indicate that macrophages play a significant role in fracture healing. Depending on the cytokine milieu, macrophages can differentiate into pro- or anti-inflammatory cells, influencing the progression of regeneration or remodeling. The regulatory patterns of macrophages represent a potential target for improving bone quality by modulating their involvement in the remodeling process of immune cells.

While this study demonstrated a correlation between NL3 and 4 gene knockouts and the expression/accumulation of M1 and M2 macrophages. Additional studies are required to comprehensively elucidate the underlying mechanisms and identify potential therapeutic targets related to macrophage polarization in ASD-associated bone metabolism disorders.

Limitations

As there are few studies similar to the present one, several limitations need to be mentioned. Animal models consistently present challenges because it is often difficult to directly apply their findings to human models. One substantiation that strengthens the possible transfer to humans is that mutations or absence of the neuronal cell surface proteins Neuroligin 3 and 4 are well-known markers for the detection or association of autistic spectrum disorder, such as Asperger Syndrome (71,72). Beyond behavioral studies in mouse models, fundamental research in neuropsychiatric disorders is essential for developing new therapeutic strategies and is currently in progress (73).

A potential critique arises from the small and uneven group sizes within the three designated groups. This situation is attributed to the acquisition of animals from a separate laboratory instead of conducting our own breeding. Moreover, the unequal distribution of male and female animals stems from the X-linked nature of the Neuroligin knockout, resulting in the availability of only male mice (73). Additionally, this study relied on animals sourced from the MPI Göttingen, which were not specifically bred for the objectives of this investigation.

Another aspect for consideration pertains to the current treatment approach adopted for affected individuals, which primarily revolves around pharmacotherapy. Consequently, the focus is predominantly on managing behavioral aspects, often overlooking physical manifestations and associated consequences, such as alterations in cellular structure suggested by the Movat Pentachrome staining. The medication regimen typically administered to individuals with ASD primarily comprises serotonin agonists, which may lead to reduced serotonin levels. Serotonin serves as a pivotal messenger in bone metabolism by regulating the equilibrium between osteogenesis and bone resorption (74). An imbalance in serotonin levels may result in diminished bone quality and elevated susceptibility to bone fractures (17,18).

The mice utilized in this study were sacrificed and examined between 12 to 16 weeks of age, which corresponds to adulthood in the literature (75). We anticipated this age range to coincide with peak bone mass. However, potential changes in bone quality, cell arrangement, or distribution with advancing age could not be assessed in this study. It is likely that bone quality may decline with age, affecting the evaluation of bone structure in ASD-affected patients. This limitation highlights the need for future investigations, potentially involving different time points and larger sample sizes. Additionally, exploring various time points and comparing them in young (6 weeks, pre-peak bone mass age),

adult (peak bone mass age), and older mice (up to 18 weeks, post-peak bone mass age) could provide valuable insights.

Regarding existing research, it is notable that ASD studies predominantly concentrate on children. There is a paucity of investigations focusing on elderly or adult patients compared to the attention given to younger individuals. However, ASD is a condition that is incurable and affects not only children but individuals across various age groups.

Conclusion

Within the scope of this study, histomorphological and enzyme histochemical alterations at the cellular level were demonstrated in the autistic mouse model, implying an influence of ASD on bone metabolism. Histomorphological examinations revealed a narrower growth plate in the femur bone of the knockout group, indicating altered bone growth. Additionally, differences in osteoclast quantity and significant disparities in osteoclast count were observed between the knockout and wild-type groups.

At the level of immune cells, changes such as an increased number of M2 macrophages were observed, indicating a dysregulation between pro- and anti-inflammatory phases.

ASD, as an apparent neurodevelopmental disease, shows potential interactions with bone metabolism. Recent studies have demonstrated that metabolic problems can occur in patients with certain orthopedic conditions, such as neurofibromatosis or diabetes mellitus. These discrepancies highlight new approaches for future studies to prevent fractures in individuals affected by ASD. Currently, no therapeutic approach exists for strengthening bone structure in individuals with ASD. Further studies and experiments are necessary to achieve a clearer understanding of metabolic activities at the cellular level. Such knowledge could be valuable in preventing bone fragility and mitigating potential complications such as fractures or early-onset osteoporosis.

7. Summary

A foundational understanding of bone metabolism at the cellular level in pre-clinical autistic models could potentially aid in preserving bone quality, given that higher fracture rates have been observed in patients with ASD.

Autism Spectrum Disorder (ASD) is not solely a neurodevelopmental condition; it also exerts significant effects on bone structure and metabolism. Several publications have documented an elevated risk of fractures in both pediatric and adult populations with ASD, alongside findings of reduced bone thickness, which correlates with an increased fracture risk (34). The risk of bone fractures in individuals with ASD may be approximately 30% to 50% higher compared to those without ASD (37). These percentages are estimates and may vary based on factors such as age, severity of ASD symptoms, comorbidities, and other individual characteristics.

Further detailed analyses are required to investigate the influence of genetic alterations on bone metabolism. Therefore, we conducted radiological, enzyme- and immunohistochemical evaluations alongside investigating macrophage activity in bone. Radiological assessments did not confirm the differences reported in the literature between wild-type and knockout groups. Histomorphometry revealed a narrowed growth plate in the NL4 knockout group. Conversely, the NL3 knockout group showed significantly increased osteoclast activity, indicating a potential imbalance in bone turnover. The percentage of osteoblasts in the NL4 knockout group was four times higher compared to the other groups. Immunohistochemically, an increased presence of immune cells was observed in the knockout groups. In the NL4 knockout group, there was an increased presence of macrophages in stage M1, suggesting a prevailing pro-inflammatory metabolic state. Initial research suggests that macrophages have a crucial role in the process of fracture healing (4,5,20). The regulatory patterns of macrophages represent a potential target for improving bone quality by modulating their involvement in the remodeling process of immune cells. Also noteworthy in histological analysis was the increased number of osteoblasts and osteoclasts in the NL3 knockout group compared to the other groups, which may have metabolic and cellular relevance.
As a prospect for future research endeavors, there is a need to focus on the qualitative properties of bone, whereas this study centered on quantitative examination of bone structure. Further intracellular investigations are now required to contextualize the observed quantitative changes in relation to a potentially poorer quality of bone structure.

Zusammenfassung

Ein grundlegendes Verständnis des Knochenstoffwechsels auf zellulärer Ebene im präklinischen autistischen Mausmodell könnte dazu beitragen, die Knochenqualität zu erhalten, da bei ASD-Patienten bereits höhere Frakturraten beobachtet wurden.

Die Autismus-Spektrum-Störung ist nicht ausschließlich eine neurologische Entwicklungsstörung, sondern wirkt sich auch signifikant auf die Knochenstruktur und den Knochenstoffwechsel aus. Mehrere Veröffentlichungen haben ein erhöhtes Risiko für Knochenbrüche sowohl bei pädiatrischen als auch erwachsenen Populationen mit ASD dokumentiert, sowie eine reduzierte Knochendicke, was mit einem erhöhten Frakturrisiko korreliert (34). Das Frakturrisiko bei Individuen mit ASD kann hier etwa 30% bis 50% höher sein im Vergleich zu denen ohne ASD (37). Diese Prozentsätze variieren je nach Faktoren wie Alter, Schwere der ASD-Symptome, Komorbiditäten und weiteren individuellen Merkmalen.

Weitere detaillierte Analysen sind erforderlich, um den Einfluss genetischer Veränderungen auf den Knochenstoffwechsel zu untersuchen. Daher führten wir radiologische, enzymatische und immunhistochemische Bewertungen durch und untersuchten gleichzeitig die Makrophagen-Aktivität im Knochen. Radiologische Untersuchungen bestätigten nicht die in der Literatur beschriebenen Unterschiede zwischen Wildtyp- und Knockout-Mäusen. Die Histomorphometrie zeigte eine schmalere Wachstumsplatte in der NL4 Knockout-Gruppe. Im Gegensatz dazu zeigte die NL3 Knockout-Gruppe eine signifikant erhöhte Aktivität von Osteoklasten, was auf ein mögliches Ungleichgewicht im Knochenstoffwechsel schließen lässt. Der prozentuale Anteil an Osteoblasten in der NL4 Knockout-Gruppe zeigte sich viermal höher im Vergleich zu den anderen Gruppen. Immunhistochemisch wurde eine erhöhte Präsenz von Immunzellen in den Knockout-Gruppen beobachtet. In der NL4 Knockout-Gruppe wurde eine erhöhte Präsenz von Makrophagen im Stadium M1 festgestellt, was auf einen vorherrschenden proinflammatorischen Stoffwechselzustand hinweist. Vorläufige Studien deuten darauf hin, dass Makrophagen eine bedeutende Rolle bei der Frakturheilung spielen (4,5,20). Die regulatorischen Muster von Makrophagen stellen ein potenzielles Ziel zur Verbesserung der Knochenqualität dar, da sie am Remodeling-Prozess von Immunzellen teilhaben. Ebenfalls nennenswert in der histologischen Analyse war die erhöhte Anzahl von Osteoblasten und Osteoklasten in der NL3-Knockout-Gruppe im Vergleich zu den anderen Gruppen, was metabolische und zelluläre Relevanz haben könnte.

Als Aussicht auf folgende Forschungsansätze ist nun ein Fokus auf die qualitativen Eigenschaften des Knochens zu setzen. Diese Arbeit ist auf die quantitative Untersuchung der Knochenstruktur fokussiert. Hier sind nun weitere Untersuchungen

notwendig, um die beobachteten quantitativen Veränderungen in Relation zu einer potenziell schlechteren Qualität der Knochenstruktur zu setzen.

8. References

1. Lyall K, Croen L, Daniels J, Fallin MD, Ladd-Acosta C, Lee BK, u. a. The Changing Epidemiology of Autism Spectrum Disorders. Annu Rev Public Health. 20. März 2017;38:81–102.
2. Neumeyer AM, Gates A, Ferrone C, Lee H, Misra M. Bone Density in Peripubertal Boys with Autism Spectrum Disorders. J Autism Dev Disord. Juli 2013;43(7):1623–9.
3. Ekhlaspour L, Baskaran C, Campoverde KJ, Sokoloff NC, Neumeyer AM, Misra M. Bone Density in Adolescents and Young Adults with Autism Spectrum Disorders. J Autism Dev Disord. November 2016;46(11):3387–91.
4. Zaidi M, Yuen T, Sun L, Rosen CJ. Regulation of Skeletal Homeostasis. Endocr Rev. 1. Oktober 2018;39(5):701–18.
5. Schlundt C, El Khassawna T, Serra A, Dienelt A, Wendler S, Schell H, u. a. Macrophages in bone fracture healing: Their essential role in endochondral ossification. Bone. Januar 2018;106:78–89.
6. Schiebler TH, Korf HW. Anatomie: Histologie, Entwicklungsgeschichte, makroskopische und mikroskopische Anatomie, Topographie ; unter Berücksichtigung des Gegenstandskatalogs. 10., vollständig überarbeitete Auflage. Darmstadt: Steinkopff Verlag; 2007. 916 S.
7. Welsch U, Kummer W, Deller T. Histologie: Zytologie, Histologie und mikroskopische Anatomie: das Lehrbuch. 5. Auflage. München: Elsevier; 2018. 734 S.
8. Christ B, Herausgeber. Anatomie. 1: Zellen- und Gewebelehre, Entwicklungslehre, Skelett- und Muskelsystem, Atemsystem, Verdauungssystem, Harn- und Genitalsystem / [unter Mitarb. von B. Christ]. 17., durchges. Aufl. München Jena: Elsevier, Urban & Fischer; 2008. 956 S.
9. Martínez-Reina J, García-Rodríguez J, Mora-Macías J, Domínguez J, Reina-Romo E. Comparison of the volumetric composition of lamellar bone and the woven bone of calluses. Proc Inst Mech Eng H. Juli 2018;232(7):682–9.
10. An YH, Martin KL, Aaron JE, Herausgeber. Handbook of histology methods for bone and cartilage. Totowa, NJ: Humana Press; 2003. 587 S.
11. Tresguerres FGF, Torres J, López-Quiles J, Hernández G, Vega JA, Tresguerres IF. The osteocyte: A multifunctional cell within the bone. Ann Anat. Januar 2020;227:151422.
12. Matic I, Matthews BG, Wang X, Dyment NA, Worthley DL, Rowe DW, u. a. Quiescent Bone Lining Cells Are a Major Source of Osteoblasts During Adulthood. Stem Cells. Dezember 2016;34(12):2930–42.
13. Udagawa N, Takahashi N, Akatsu T, Tanaka H, Sasaki T, Nishihara T, u. a. Origin of osteoclasts: mature monocytes and macrophages are capable of differentiating into osteoclasts under a suitable microenvironment prepared by bone marrow-derived stromal cells. Proc Natl Acad Sci U S A. September 1990;87(18):7260–4.
14. Rupp M, Merboth F, Daghma D, Biehl C, El Khassawna T, Heiß C. Osteocytes: Osteocytes in Bone Remodeling – Conductors and Active Players. Z Orthop Unfall. April 2019;157(02):154–63.
15. Kylmaoja E, Nakamura M, Tuukkanen J. Osteoclasts and Remodeling Based Bone Formation. Curr Stem Cell Res Ther. 2016;11(8):626–33.
16. Ernst L, Casals E, Italiani P, Boraschi D, Puntes V. The Interactions between Nanoparticles and the Innate Immune System from a Nanotechnologist Perspective. Nanomaterials. 6. November 2021;11(11):2991.

17. Abbas AK, Lichtman AH, Pober JS. Cellular and molecular immunology. Philadelphia: Saunders; 1991. 417 S.
18. Janeway C, Herausgeber. Immunobiology: the immune system in health and disease ; [animated CD-ROM inside]. 5. ed. New York, NY: Garland Publ. [u.a.]; 2001. 732 S.
19. Wang Y, Lin Q, Zhang H, Wang S, Cui J, Hu Y, u. a. M2 macrophage-derived exosomes promote diabetic fracture healing by acting as an immunomodulator. Bioact Mater. Oktober 2023;28:273–83.
20. Wang W, Liu H, Liu T, Yang H, He F. Insights into the Role of Macrophage Polarization in the Pathogenesis of Osteoporosis. Nagai R, Herausgeber. Oxidative Medicine and Cellular Longevity. 6. Juni 2022;2022:1–11.
21. Schlundt C, Fischer H, Bucher CH, Rendenbach C, Duda GN, Schmidt-Bleek K. The multifaceted roles of macrophages in bone regeneration: A story of polarization, activation and time. Acta Biomater. 1. Oktober 2021;133:46–57.
22. Kamp-Becker I, Bölte S. Autismus. 3., vollständig überarbeitete Auflage. München: Ernst Reinhardt Verlag; 2021. 111 S. (UTB Psychologie, Pädagogik).
23. Deutsche Gesellschaft für Kinder- und Jugendpsychiatrie, Psychosomatik und Psychotherapie. S3-Leitlinie Autismus-Spektrum-Störungen im Kindes-, Jugend- und Erwachsenenalter. AWMF; 2021.
24. American Psychiatric Association, American Psychiatric Association, Herausgeber. Diagnostic and statistical manual of mental disorders: DSM-5. 5th ed. Washington, D.C: American Psychiatric Association; 2013. 947 S.
25. Qiu S, Qiu Y, Li Y, Cong X. Genetics of autism spectrum disorder: an umbrella review of systematic reviews and meta-analyses. Transl Psychiatry. 15. Juni 2022;12(1):249.
26. Wang L, Wang B, Wu C, Wang J, Sun M. Autism Spectrum Disorder: Neurodevelopmental Risk Factors, Biological Mechanism, and Precision Therapy. Int J Mol Sci. 17. Januar 2023;24(3):1819.
27. Maxeiner S, Benseler F, Krasteva-Christ G, Brose N, Südhof TC. Evolution of the Autism-Associated Neuroligin-4 Gene Reveals Broad Erosion of Pseudoautosomal Regions in Rodents. Nowick K, Herausgeber. Molecular Biology and Evolution. 1. Mai 2020;37(5):1243–58.
28. Zhang B, Gokce O, Hale WD, Brose N, Südhof TC. Autism-associated neuroligin-4 mutation selectively impairs glycinergic synaptic transmission in mouse brainstem synapses. J Exp Med. 4. Juni 2018;215(6):1543–53.
29. Rawsthorne H, Calahorro F, Feist E, Holden-Dye L, O'Connor V, Dillon J. Neuroligin dependence of social behaviour in Caenorhabditis elegans provides a model to investigate an autism-associated gene. Hum Mol Genet. 6. Januar 2021;29(21):3546–53.
30. Amodeo DA, Oliver B, Pahua A, Hitchcock K, Bykowski A, Tice D, u. a. Serotonin 6 receptor blockade reduces repetitive behavior in the BTBR mouse model of autism spectrum disorder. Pharmacology Biochemistry and Behavior. Januar 2021;200:173076.
31. Arberas C, Ruggieri V. [Autism. Genetic and biological aspects]. Medicina (B Aires). 2019;79(Suppl 1):16–21.
32. Dziobek I, Stoll S. Hochfunktionaler Autismus bei Erwachsenen: ein kognitiv-verhaltenstherapeutisches Manual. 1. Auflage. Stuttgart: Verlag W. Kohlhammer; 2019. 196 S. (Kohlhammer Manuale).
33. Turner M. The role of drugs in the treatment of autism. Aust Prescr. Dezember 2020;43(6):185–90.

34. Neumeyer AM, O'Rourke JA, Massa A, Lee H, Lawson EA, McDougle CJ, u. a. Brief report: bone fractures in children and adults with autism spectrum disorders. J Autism Dev Disord. März 2015;45(3):881–7.
35. Rostami Haji Abadi M, Neumeyer A, Misra M, Kontulainen S. Bone health in children and youth with ASD: a systematic review and meta-analysis. Osteoporos Int. September 2021;32(9):1679–91.
36. Neumeyer AM, Cano Sokoloff N, McDonnell E, Macklin EA, McDougle CJ, Misra M. Bone microarchitecture in adolescent boys with autism spectrum disorder. Bone. April 2017;97:139–46.
37. Whitney DG, Caird MS, Jepsen KJ, Kamdar NS, Marsack-Topolewski CN, Hurvitz EA, u. a. Elevated fracture risk for adults with neurodevelopmental disabilities. Bone. Januar 2020;130:115080.
38. Gładysz D, Krzywdzińska A, Hozyasz KK. Immune Abnormalities in Autism Spectrum Disorder-Could They Hold Promise for Causative Treatment? Mol Neurobiol. August 2018;55(8):6387–435.
39. Aldossari AA, Ansari MA, Nadeem A, Attia SM, Bakheet SA, Al-Ayadhi LY, u. a. Upregulation of Inflammatory Mediators in Peripheral Blood CD40+ Cells in Children with Autism Spectrum Disorder. IJMS. 19. April 2023;24(8):7475.
40. Meltzer A, Van de Water J. The Role of the Immune System in Autism Spectrum Disorder. Neuropsychopharmacology. Januar 2017;42(1):284–98.
41. Tabuchi K, Blundell J, Etherton MR, Hammer RE, Liu X, Powell CM, u. a. A neuroligin-3 mutation implicated in autism increases inhibitory synaptic transmission in mice. Science. 5. Oktober 2007;318(5847):71–6.
42. Bryant CD. The blessings and curses of C57BL/6 substrains in mouse genetic studies. Ann N Y Acad Sci. Dezember 2011;1245:31–3.
43. Kang SK, Hawkins NA, Kearney JA. C57BL/6J and C57BL/6N substrains differentially influence phenotype severity in the Scn1a +/- mouse model of Dravet syndrome. Epilepsia Open. März 2019;4(1):164–9.
44. Brown SDM, Moore MW. Towards an encyclopaedia of mammalian gene function: the International Mouse Phenotyping Consortium. Disease Models & Mechanisms. 1. Mai 2012;5(3):289–92.
45. Mattapallil MJ, Wawrousek EF, Chan CC, Zhao H, Roychoudhury J, Ferguson TA, u. a. The Rd8 mutation of the Crb1 gene is present in vendor lines of C57BL/6N mice and embryonic stem cells, and confounds ocular induced mutant phenotypes. Invest Ophthalmol Vis Sci. 2012;53(6):2921–7.
46. Shi J, Lee S, Uyeda M, Tanjaya J, Kim JK, Pan HC, u. a. Guidelines for Dual Energy X-Ray Absorptiometry Analysis of Trabecular Bone-Rich Regions in Mice: Improved Precision, Accuracy, and Sensitivity for Assessing Longitudinal Bone Changes. Tissue Engineering Part C: Methods. Mai 2016;22(5):451–63.
47. Biehl C, Schmitt J, Stoetzel S, Malhan D, Hassan F, Knapp G, u. a. DXA reference values of the humanoid sheep model in preclinical studies. PeerJ. 30. April 2021;9:e11183.
48. Malhan D, Muelke M, Rosch S, Schaefer AB, Merboth F, Weisweiler D, u. a. An Optimized Approach to Perform Bone Histomorphometry. Front Endocrinol. 21. November 2018;9:666.
49. Dittfeld C, Haase M, Feilmeier M, Jannasch A, Büttner P, Plötze K, u. a. Movat Pentachrom stain reveals unexpected high osteogenesis rate in aortic valves. Acta Histochem. Juni 2017;119(5):533–7.
50. Movat HZ. Tissue injury and inflammation induced by immune complexes: the critical role of the neutrophil leukocyte. Experimental and Molecular Pathology. August

1979;31(1):201–10.
51. Olah AJ, Simon A, Gaudy M, Herrmann W, Schenk RK. Differential staining of calcified tissues in plastic embedded microtome sections by a modification of Movat's pentachrome stain. Stain Technol. November 1977;52(6):331–7.
52. Lojda Z, Gossrau R, Schiebler TH, Lojda Z, Gossrau R, Schiebler TH, u. a. Enzyme histochemistry: a laboratory manual. Berlin Heidelberg: Springer; 1979. 339 S.
53. Hayman AR. Tartrate-resistant acid phosphatase (TRAP) and the osteoclast/immune cell dichotomy. Autoimmunity. April 2008;41(3):218–23.
54. Filgueira L. Fluorescence-based staining for tartrate-resistant acidic phosphatase (TRAP) in osteoclasts combined with other fluorescent dyes and protocols. J Histochem Cytochem. März 2004;52(3):411–4.
55. Ballanti P, Minisola S, Pacitti MT, Scarnecchia L, Rosso R, Mazzuoli GF, u. a. Tartrate-resistant acid phosphate activity as osteoclastic marker: sensitivity of cytochemical assessment and serum assay in comparison with standardized osteoclast histomorphometry. Osteoporos Int. 1997;7(1):39–43.
56. Kumar, Rudbeck G Lars. Immunohistochemical Staining Methods, Fifth Version. Dako, North America; 2009.
57. Ducy P, Desbois C, Boyce B, Pinero G, Story B, Dunstan C, u. a. Increased bone formation in osteocalcin-deficient mice. Nature. 1. August 1996;382(6590):448–52.
58. Bailey S, Karsenty G, Gundberg C, Vashishth D. Osteocalcin and osteopontin influence bone morphology and mechanical properties. Ann N Y Acad Sci. Dezember 2017;1409(1):79–84.
59. Chistiakov DA, Killingsworth MC, Myasoedova VA, Orekhov AN, Bobryshev YV. CD68/macrosialin: not just a histochemical marker. Lab Invest. Januar 2017;97(1):4–13.
60. Mir MA. Developing costimulatory molecules for immunotherapy of diseases. Amsterdam: Elsevier/Academic Press; 2015.
61. Arganda-Carreras I, Kaynig V, Rueden C, Eliceiri KW, Schindelin J, Cardona A, u. a. Trainable Weka Segmentation: a machine learning tool for microscopy pixel classification. Bioinformatics. 1. August 2017;33(15):2424–6.
62. Pecorelli A, Cordone V, Schiavone ML, Caffarelli C, Cervellati C, Cerbone G, u. a. Altered Bone Status in Rett Syndrome. Life. 3. Juni 2021;11(6):521.
63. Devlin MJ, Rosen CJ. The bone–fat interface: basic and clinical implications of marrow adiposity. The Lancet Diabetes & Endocrinology. Februar 2015;3(2):141–7.
64. Bell-Hensley A, Beard DC, Feeney K, Zheng H, Jiang Y, Zhang X, u. a. Skeletal abnormalities in mice with Dnmt3a missense mutations. Bone. Juni 2024;183:117085.
65. Tiede-Lewis LM, Dallas SL. Changes in the osteocyte lacunocanalicular network with aging. Bone. Mai 2019;122:101–13.
66. Komori T. Functions of the osteocyte network in the regulation of bone mass. Cell Tissue Res. Mai 2013;352(2):191–8.
67. El Khassawna T, Böcker W, Brodsky K, Weisweiler D, Govindarajan P, Kampschulte M, u. a. Impaired extracellular matrix structure resulting from malnutrition in ovariectomized mature rats. Histochem Cell Biol. November 2015;144(5):491–507.
68. Fischer V, Haffner-Luntzer M. Interaction between bone and immune cells: Implications for postmenopausal osteoporosis. Semin Cell Dev Biol. März 2022;123:14–21.
69. Mu H, Jia H, Lin ZH, Zheng HH, Wang L, Liu H. [Role of imbalance of M1/M2 subsets of bone marrow macrophages in the pathogenesis of immune-mediated aplastic anemia in mice]. Zhonghua Xue Ye Xue Za Zhi. 14. November 2021;42(11):945–51.

70. Minkwitz S, Faßbender M, Kronbach Z, Wildemann B. Longitudinal Analysis of Osteogenic and Angiogenic Signaling Factors in Healing Models Mimicking Atrophic and Hypertrophic Non-Unions in Rats. Shi XM, Herausgeber. PLoS ONE. 24. April 2015;10(4):e0124217.
71. Gogolla N, Leblanc JJ, Quast KB, Südhof TC, Fagiolini M, Hensch TK. Common circuit defect of excitatory-inhibitory balance in mouse models of autism. J Neurodev Disord. Juni 2009;1(2):172–81.
72. Bey AL, Jiang YH. Overview of mouse models of autism spectrum disorders. Curr Protoc Pharmacol. 2. September 2014;66:5.66.1-5.66.26.
73. Unichenko P, Yang JW, Kirischuk S, Kolbaev S, Kilb W, Hammer M, u. a. Autism Related Neuroligin-4 Knockout Impairs Intracortical Processing but not Sensory Inputs in Mouse Barrel Cortex. Cereb Cortex. 1. August 2018;28(8):2873–86.
74. Lavoie B, Lian JB, Mawe GM. Regulation of Bone Metabolism by Serotonin. Adv Exp Med Biol. 2017;1033:35–46.
75. Mattapallil MJ, Wawrousek EF, Chan CC, Zhao H, Roychoudhury J, Ferguson TA, u. a. The *Rd8* Mutation of the *Crb1* Gene Is Present in Vendor Lines of C57BL/6N Mice and Embryonic Stem Cells, and Confounds Ocular Induced Mutant Phenotypes. Invest Ophthalmol Vis Sci. 17. Mai 2012;53(6):2921.

9. Appendixes

List of figures

List of tables

List of reagents with source of supply

Paraffin Embedding and Dehydration procedure:

Material	
Ethanol 100%	Herbeta drug, Berlin, Germany *Methyl Ethyl Ketone (MEK) denatured
EDTA	EDTA decalcifying solution, Herbeta Drug, Berlin, Germany
Paraffin	Leica Microsystems, Nussloch GmbH Germany EG1120
PFA	4 % W/V Parafromaldehyde powder in DEPC treated water, pH 9.1

Movat Pentachrome Staining:

Material	
Alcian blue-solution	Laboratories Croma, Ueberlingen, Germany, Nr. 2C-005
Weigert's Iron Hematoxylin solution	Laboratories Roth, Karlsruhe, Germany, Nr. X906, Nr. X907
Brilliant Crocein – Acid Fuchsine solution	Laboratories Croma, Ueberlingen, Germany, Nr. 1B-109
Saffron du gatinais solution	Laboratories Croma, Ueberlingen, Germany, Nr. 5A-394
Vitro-Clud	Laboratories R. Langenbrinck (Emmendingen, Germany)

Tartrate-Resistant Acid Phosphatase (TRAP) Staining:

Material	
Naphthol-AS-TR-Phosphat	Sigma Aldrich Chemie GmbH, Steinheim, Germany, Nr. N6125
N-N-Dimethylformamid	Sigma Aldrich Chemie GmbH, Steinheim, Germany, Nr. D4551
di-Natriumtartrat-Dihydrat	Merck KGaA, Darmstadt, Germany, Nr. 1.06663

Echtrotsalz (Fast Red TR Salt)	Sigma Aldrich Chemie GmbH, Steinheim, Germany, Nr. 368881
Sodium acetate buffer	Merck KGaA, Darmstadt, Germany, Nr. 1-062680
Instant Hematoxylin	Thermo Scientific, Nr. 6765015
Vitro-Clud	Laboratories R. Langenbrinck (Emmendingen, Germany)

Immunohistochemical Staining

Material	
ABC-AP kit	Alkaline phosphatase, AK5200 Universal kit, Vectastain ABC kit, Vector Laboratories, Inc., Burlingame, CA, USA
AP-substrate kit	Vector® Red Alkaline phosphatase substrate, SK-5100, Vector Laboratories Inc., Burlingame, CA, USA
Bloxal Blocking Solution	Vector Laboratories, Inc., SP-6000, Burlinghame, CA, USA
CD68 (1:200)	Primary antibody, rabbit polyclonal, ab125212, Abcam, Cambridge, MA, USA
CD80 (1:200)	Primary antibody, rabbit polyclonal, ab64116, Abcam, Cambridge, MA, USA
CD206 (1:500)	Primary antibody, rabbit polyclonal, ab64693, Abcam, Cambridge, MA, USA
Osteocalcin (1:1500)	Primary antibody, rabbit polyclonal, ab93876, Abcam, Cambridge, MA, USA
Citrate buffer	Citrate acid monohydrate, 3958.2, Carl Roth GmbH, Karlsruhe, Germany; tri-Sodium citrate hydrate, 1.06448.1000, Merck KGaA, Darmstadt, Germany
Glacial acetic acid	Glacial Acetic acid (EC Number 2005807, Merck, Darmstadt, Germany)
Methyl green	Methyl green, H-3402, Vector Laboratories Inc., Burlingame, CA, USA
TBS	TRIS Pufferan®, 4855.2, Carl Roth GmbH, Karlsruhe, Germany; Sodium chloride, 31434-1KG-R, Sigma Aldrich Chemie GmbH, Steinheim, Germany; Hydrochloric acid 25%, 1.00316.1011, Merck KGaA, Darmstadt, Germany

Abbreviations list

[%]	Percentage
[°C]	Degree Celsius
AP	Alkaline Phosphatase
ASD	Autism Spectrum Disorder
BMC	Bone Mineral Content
BMD	Bone Mineral Density
BMU	Basic/Bone Multicellular Unit
CD 68	immunohistochemical marker for macrophages
CD 80	immunohistochemical marker for M1 macrophages
CD 206	immunohistochemical marker for M2 macrophages
CM	centimetre
D	Day
DNMT3A	DNA methyltransferase 3A
DXA	Dual-Energy X-Ray Absorptiometry
ECM	Extracellular Matrix
IHC	Immunohistochemistry
OCN	Osteocalcin
DSM-V	Diagnostic and Statistical Manual of Mental Disorders
MECP2	Methyl-CpG-binding Protein 2
MG	milligram
MM	millimetre
MPS	Mononuclear Phagocytic System
NL	Neuroligin
NLGN3	Neuroligin 3
NLGN4	Neuroligin 4
PDD-NOS	Pervasive Developmental Disorder – Not Otherwise Specified
PFA	Paraformaldehyde
RT	Room temperature
TRAP	Tartrate-resistant Acid Phosphatase
WT	wild type

10. Thesis declaration

Erklärung zur Dissertation

„Hiermit erkläre ich, dass ich die vorliegende Arbeit selbständig und ohne unzulässige Hilfe oder Benutzung anderer als der angegebenen Hilfsmittel angefertigt habe. Alle Textstellen, die wörtlich oder sinngemäß aus veröffentlichten oder nichtveröffentlichten Schriften entnommen sind, und alle Angaben, die auf mündlichen Auskünften beruhen, sind als solche kenntlich gemacht. Bei den von mir durchgeführten und in der Dissertation erwähnten Untersuchungen habe ich die Grundsätze guter wissenschaftlicher Praxis, wie sie in der „Satzung der Justus-Liebig-Universität Gießen zur Sicherung guter wissenschaftlicher Praxis“ niedergelegt sind, eingehalten sowie ethische, datenschutzrechtliche und tierschutzrechtliche Grundsätze befolgt. Ich versichere, dass Dritte von mir weder unmittelbar noch mittelbar geldwerte Leistungen für Arbeiten erhalten haben, die im Zusammenhang mit dem Inhalt der vorgelegten Dissertation stehen, oder habe diese nachstehend spezifiziert. Die vorgelegte Arbeit wurde weder im Inland noch im Ausland in gleicher oder ähnlicher Form einer anderen Prüfungsbehörde zum Zweck einer Promotion oder eines anderen Prüfungsverfahrens vorgelegt. Alles aus anderen Quellen und von anderen Personen übernommene Material, das in der Arbeit verwendet wurde oder auf das direkt Bezug genommen wird, wurde als solches kenntlich gemacht. Insbesondere wurden alle Personen genannt, die direkt und indirekt an der Entstehung der vorliegenden Arbeit beteiligt waren. Mit der Überprüfung meiner Arbeit durch eine Plagiatserkennungssoftware bzw. ein internetbasiertes Softwareprogramm erkläre ich mich einverstanden.“

_____ _____ Ort,

Datum Unterschrift

11. Acknowledgments

12. Curriculum Vitae